

Matrix parameterization of the 15 μm CO_2 band cooling in the middle and upper atmosphere for variable CO_2 concentration

V.I. Fomichev^{1,2} and J.-P. Blanchet

Earth Sciences Department, Université du Québec à Montréal, Montréal, Canada

D. S. Turner

Meteorological Research Branch, Atmospheric Environment Service, Toronto, Canada

Abstract. A matrix parameterization of the 15 μm CO_2 band radiative cooling in the middle and upper terrestrial atmosphere for both local thermodynamic equilibrium (LTE) and non-LTE (NLTE) layers is proposed. For the atmospheric region between ~ 13 and 85 km, matrix coefficients for CO_2 concentrations of 150, 360, 540, and 720 ppm have been precalculated using a line-by-line technique. A method for interpolation of the matrix coefficients for arbitrary CO_2 concentration is suggested. In the layer between 85 and 110 km, where strong NLTE effects start to occur, a recurrence formula relating cooling rate values at two neighboring altitude levels is used. To calculate the cooling rate above 110 km, a simple approach accounting for both the absorption of the radiative flux formed below 110 km and the cooling-to-space terms is suggested. The accuracy of the parameterization is examined for different temperature and CO_2 profiles as well as for different atomic oxygen concentrations in the NLTE layer.

1. Introduction

Among the important open questions facing atmospheric scientists today is what effect anthropogenically generated increases of CO_2 concentration in the atmosphere will have on the Earth's atmosphere. Investigation of this question is not limited to the troposphere but includes the stratosphere, mesosphere, and lower thermosphere. Although the "greenhouse effect," as this is often called, involves heating of the troposphere, other regions of the atmosphere are significantly cooled [e.g., Fels *et al.*, 1980; Rishbeth and Roble, 1992]. To investigate the effect of changes in the CO_2 concentration using three-dimensional (3-D) atmospheric models, a radiation code capable of quickly and accurately calculating the CO_2 cooling rate over a range of heights, temperatures, and CO_2 concentrations is needed. In this paper, such a code is presented and described.

Radiative cooling in the 15 μm CO_2 band is one of the basic processes which determines the Earth's cli-

mate and its changes. The calculation of cooling rates in the middle atmosphere is a widely investigated problem which still consumes a lot of computer time. Complete descriptions of the problem and approaches to its solution have been presented by several authors [e.g., Andreus *et al.*, 1987]. The most expensive part in computing the cooling rate is the calculation of the absorption characteristics of the spectral bands taking into account the effects of atmospheric inhomogeneity. In addition, above ~ 70 km the breakdown of local thermodynamic equilibrium (LTE) conditions in the 15 μm CO_2 band must be taken into account, rendering the calculations more complex. Thus providing parameterizations for the 15 μm CO_2 band cooling rate is an essential part of the development of modern comprehensive dynamical models.

To adequately account for radiative cooling in these dynamical models, an ideal parameterization must satisfy the following conditions: (1) it must be computationally efficient; (2) it must be accurate for the purposes of the model; and (3) it must easily allow for feedbacks by ensuring that the dependencies on all input parameters (temperature, atmospheric composition, and the rate constants for collisional quenching of the vibrational states) are easily taken into account. Unfortunately it is not possible to completely satisfy all these requirements at once. There is always a compromise between computational efficiency, on the one hand, and accuracy and flexibility, on the other hand. Depending on the complexity of the dynamical model and on the

¹On leave from Atmospheric Physics Department, Institute of Physics, University of St. Petersburg, Russia.

²Now at Department of Earth and Atmospheric Science, York University, Toronto, Canada.

Copyright 1998 by the American Geophysical Union.

Paper number 98JD00799.
0148-0227/98/98JD-00799\$09.00

problem at hand, a suitable compromise may be chosen for each case.

All existing parameterizations can be classified into two major groups. The first group consists of parameterizations employing simplified methods for solving the radiative transfer equation. In this case, cooling rates in the 15 μm CO₂ band ϵ are calculated from some standard expressions for ϵ , and the absorption characteristics, such as transmission functions, band absorbances, atmospheric emissivities, and absorptivities, are evaluated utilizing simplified analytical formulae or numerical procedures. Such an approach allows the variation of all input atmospheric parameters to be easily taken into account. The parameterizations suggested by *Apruzese et al.* [1984] for both LTE and non-LTE (NLTE) layers and by *Chou and Kouvaris* [1991], *Kiehl and Briegleb* [1991], and *Briegleb* [1992] for LTE layer are examples of this group. The main disadvantage of these parameterizations is a relatively large computational overhead, especially in the NLTE region. This makes their implementations into comprehensive 3-D models of the middle and upper atmosphere, where NLTE treatment is required, almost impossible at the moment.

The second group of parameterizations are the so-called matrix parameterizations [e.g., *Wehrbein and Leovy*, 1982; *Akmaev and Shved*, 1982; *Zhu*, 1990, 1994; *Fomichev et al.*, 1993; *Fomichev and Blanchet*, 1995]. All these schemes, except the one suggested by *Akmaev and Shved* [1982], include consideration of the NLTE layer. This type of parameterization allows the cooling rate to be calculated directly without numerical differencing or integration, and hence these parameterizations are at least an order of magnitude faster than those in group one. Because of their speed and sufficient accuracy, matrix type parameterizations are desirable for application in comprehensive 3-D models of the middle and upper atmosphere [*Haus*, 1986; *Grinkevich and Fomichev*, 1993]. However, this type of parameterization is, as a rule, less flexible because the parameterization (Curtis) matrices are usually calculated on a certain height grid and for some fixed temperature and atmospheric composition profiles.

Parameterizations by *Wehrbein and Leovy* [1982] and *Zhu* [1990, 1994] suggest utilizing a set of Curtis matrices calculated for a fixed set of temperature profiles and for a specific atmospheric composition. To obtain ϵ for an arbitrary temperature profile, matrix interpolation is used, which slows down the calculation. Moreover, in order to evaluate ϵ for different atmospheric composition a new set of Curtis matrices must be calculated.

Akmaev and Shved [1982] developed a matrix parameterization of the 15 μm CO₂ band for the LTE layer and suggested a parameterization formula with the temperature dependence specified in an explicit form. This avoided matrix interpolation and accelerated calculations. *Fomichev et al.* [1993] extended the parameterization of *Akmaev and Shved* [1982] down to the tropopause and up into the NLTE layer. The simple recurrence formula by *Kutepov and Fomichev* [1993] was

utilized in the NLTE layer. This formula links the values of ϵ at two neighboring altitude levels thereby making it possible to easily take account of variations in temperature, [O], [O₂], and [N₂] and to vary the value of the rate constants for the collisional quenching of the vibrationally excited CO₂ molecule. Finally, *Fomichev and Blanchet* [1995] simplified the parameterization formula of *Akmaev and Shved* [1982], combined the parameterization for the 15 μm CO₂ band with that for the 9.6 μm O₃ band [*Fomichev and Blanchet*, 1995], and merged this combined scheme with the tropospheric longwave radiation model of *Morcrette* [1984]. The matrix parameterizations of *Fomichev et al.* [1993] and *Fomichev and Blanchet* [1995] have been successfully implemented and utilized in several different 3-D and comprehensive 2-D dynamical models [*Akmaev et al.*, 1992; *Berger and Dameris*, 1993; *Roble and Ridley*, 1994; *Beagley et al.*, 1997; *Chen et al.*, 1997]. The main advantage of these parameterizations is that they provide formulae for cooling rate with explicit dependencies on temperature, atmospheric composition, and quenching rate constants, which makes it easy to take account of variations in input atmospheric parameters. The main disadvantage is that these parameterizations were developed using a fixed CO₂ volume mixing ratio profile c_{CO_2} , which restricts their application to investigations of the current climate.

Reporting on a new matrix parameterization applicable to a variable CO₂ concentration is the main purpose of this paper. For this parameterization the approach suggested by *Fomichev et al.* [1993] and *Fomichev and Blanchet* [1995] was generalized to a wide range of CO₂ concentration (150–720 ppm). The parameterization is based on and tested against reference cooling rate calculations utilizing a newly developed line-by-line radiative transfer model for LTE and an updated version of the *Kutepov and Shved* [1978] method for NLTE layers. The accuracy of the present parameterization, especially in LTE region, has been substantially improved in comparison to that of our previous schemes. For application in dynamical models which include treatment of the tropospheric processes, we recommend merging our scheme with tropospheric longwave radiation models using the approach suggested by *Fomichev and Blanchet* [1995].

The dimensionless log-pressure height

$$x = \log \frac{1000}{p} \quad (1)$$

where p is the pressure in mbar, is used as a vertical coordinate throughout the study. Figure 1 shows the relationship between log-pressure and geometrical heights for all climatological temperature models utilized to develop and test the parameterization. To a first approximation this relation can be expressed as $z(\text{km}) \approx 7x$.

Section 2 of the paper describes the reference methods used in order to develop and test the parameterization for both LTE and NLTE layers. The input atmospheric parameters such as temperature, CO₂, O, O₂, and N₂ concentrations are presented in section 3. Approaches utilized in creating the parameterization are

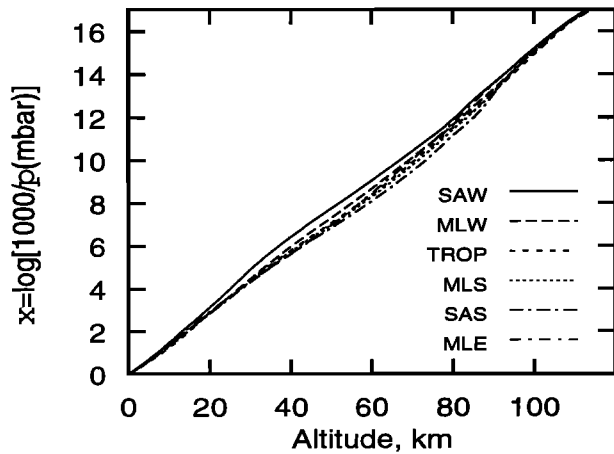


Figure 1. Relationship between log-pressure and geometrical coordinates derived for the temperature models taken from the COSPAR International Reference Atmosphere (CIRA)-1986 model and utilized to develop and test the parameterization (see Figure 4a). The abbreviations are defined as follows: SAW, Subarctic winter (June, 70°S); MLW, midlatitude winter (June, 40°S); TROP, tropics (June, equator); MLS, midlatitude summer (June, 40°N); SAS, Subarctic summer (June, 70°N); and MLE, midlatitude equinox (September, 40°N).

discussed in section 4. Section 5 provides an analysis of the accuracy of the parameterization for differing temperature, O, and CO₂ models. In the LTE layer, two versions of the parameterization utilizing different height grids to account for the internal heat exchange have been developed. The first scheme is based on a grid with uniform height step $\Delta x = 0.25$ ($\Delta z \approx 1.7$ km). Employing the method of matrix transformation suggested by *Akmaev and Fomichev* [1992], the uniform grid parameterization can be adopted for any height grid appropriate for a given dynamical model. The second scheme utilizes an optimized variable height step, the value of which increases with increasing distance from the level for which cooling is calculated. The scheme with the optimized height grid requires fewer parameterization coefficients, which makes the parameterization more computationally efficient in comparison to the scheme with the uniform vertical grid. A complete description of the scheme with the optimized height grid is presented in section 6. Section 7 summarizes the main results.

2. Reference Method

In order to develop and test the parameterization we have created a reference method for the calculation of ϵ . It consists of two parts. In the LTE layer, below $x = 10$ ($z \approx 70$ km), a line-by-line technique was applied to account for the spectral line overlapping. In the upper part of the domain, NLTE treatment with the assumption of nonoverlapping spectral lines was utilized. The values for ϵ obtained by these methods were merged

in the layer between $x = 10$ and $x = 11$ ($z \approx 70$ and $z \approx 76$ km). In this section we discuss the main features of both the line-by-line and the NLTE methods used in the reference calculation.

2.1. Line-by-Line Calculation in the LTE Layer

The line-by-line spectral code General Atmospheric Spectral Integration Suite (GENASIS) [*Drummond et al.*, 1993] was used to evaluate the mean diffuse transmission matrices for the 15 μm CO₂ band. Each of these matrices contains all the possible diffuse transmittances between any two levels of the atmosphere. These levels are defined by $x = 0-14.125$ at 0.125 intervals.

The mean diffuse transmittance matrices used to develop the parameterization are 10 cm^{-1} averages. They are created by integrating across a set of wavenumber dependent diffuse transmittance matrices on a 0.002 cm^{-1} grid. The diffuse transmittance of each matrix element is explicitly evaluated using the third exponential function applied to the total optical depth between the levels represented by the matrix element. The total optical depth is the sum of the optical depths of each contributing layer which is the product of the layer's absorption coefficient and the absorber amount. The absorption coefficient is evaluated using the layer's absorber amount weighted pressure and temperature applied to all contributing spectral lines. A contributing line is one that is within 385 Lorentz halfwidths of the matrix's position in wavenumber space. All spectral lines are assumed to be Voigt. The spectral parameters of the CO₂ lines are taken from the HITRAN-92 spectral database [*Rothman et al.*, 1992]. In total, 26 mean diffuse matrices from 540 to 800 cm^{-1} are obtained for each set of input atmospheric parameters (see section 3).

The LTE cooling rates are calculated using a standard method [e.g., *Andrews et al.*, 1987]. The cooling rates were obtained with the atmospheric region defined by $x = 2-11$ ($z \approx 13-76$ km) on a $\Delta x = 0.25$ ($\Delta z \approx 1.7$ km) grid taking into consideration the internal heat exchange within $x = 0-14$ ($z \approx 0-93$ km). The upward and downward fluxes were calculated using trapezoidal integration on a $\Delta x = 0.125$ ($\Delta z \approx 0.85$ km) grid. The radiative flux divergence is evaluated by a finite difference method on a $\Delta x = 0.5$ ($\Delta z \approx 3.4$ km) grid.

The above calculations were validated against the results of *Schwarzkopf and Fels* [1985]. A comparison between the two methods is shown in Figure 2. The cooling rate differences between our method and that of *Schwarzkopf and Fels* [1985] do not exceed 0.15 K d^{-1} and are probably due to differences between the two models.

Unlike our calculations, *Schwarzkopf and Fels* [1985] used data from the Air Force Geophysics Laboratory (AFGL)-80 spectral database [*Rothman*, 1981] and combined lines <0.01 cm^{-1} apart with a weighted line width and summed line strength. In addition, they included only those lines within 3 cm^{-1} of a wavenumber grid point, assumed a Voigt profile above 100 mbar (Lorentz otherwise), and performed a four-point Gaus-

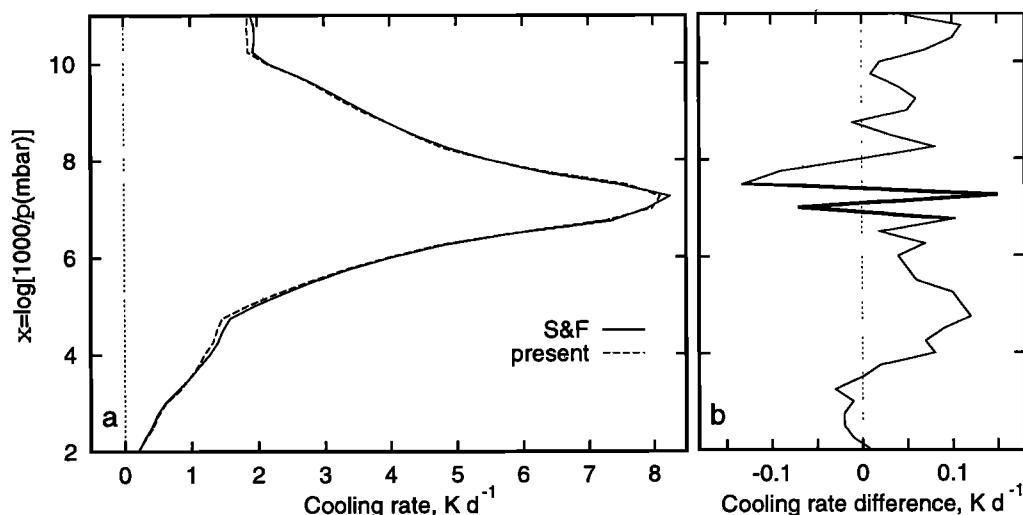


Figure 2. Comparison of the 15 μm CO₂ band radiative cooling rate in the local thermodynamic equilibrium (LTE) layer: S&F, line-by-line calculation by *Schwarzkopf and Fels* [1985] and present, present line-by-line method. (a) Cooling rate profiles and (b) difference between S&F and present method.

sian quadrature for the angular integration. Our method explicitly performs the angular integration prior to the spectral integration. Finally, the vertical numerical integration and differentiation was performed on a different vertical grid, $\Delta x \approx 0.155$ ($\Delta z \approx 1.1$ km).

2.2. NLTE Treatment

Above $x \approx 10$ ($z \approx 70$ km) the density of the atmosphere is low and the collisions between molecules are so infrequent that the populations of the excited vibrational levels are no longer controlled by the collisional processes alone. This means that the Boltzmann distribution law is not valid, and in contrast to LTE condition, the source function S is not equal to the Planck function B . In this case, to obtain S for some vibrational transition, one must solve the integral equation for an optically inhomogeneous medium (see *Kutepov and Shved* [1978] and *Kutepov and Fomichev* [1993] for details). In order to calculate ϵ one needs to obtain the source function for every contributing vibrational transition of the 15 μm CO₂ band. In our calculation we chose to use a nonoverlapping spectral line model and accounted for 14 vibrational transitions: the fundamental transitions 01^10 - 00^00 of the $^{12}\text{C}^{16}\text{O}_2$, $^{13}\text{C}^{16}\text{O}_2$, $^{12}\text{C}^{16}\text{O}^{18}\text{O}$, and $^{12}\text{C}^{16}\text{O}^{17}\text{O}$ molecules, the first-order [02^00 - 01^10 , 02^20 - 01^10 , 10^00 - 01^10], and the second-order [03^10 - 02^00 , 03^10 - 02^20 , 03^10 - 10^00 , 03^30 - 02^20 , 11^10 - 02^00 , 11^10 - 02^20 , 11^10 - 10^00] hot transitions of the $^{12}\text{C}^{16}\text{O}_2$ molecule.

To calculate the values of ϵ in the NLTE layer, a method based on the approach suggested by *Kutepov and Shved* [1978] was used. The band strengths of the vibrational transitions, as well as data on the frequencies and energy levels of the vibrational transitions comprising the 15 μm CO₂ band, were taken from the HITRAN-92 database [*Rothman et al.*, 1992]. The Voigt line shape with constant Doppler γ_D and Lorentz

γ_L halfwidths for all lines was assumed ($\gamma_L(300\text{K}) = 0.07368 \text{ cm}^{-1}$ at $p = 1\text{atm}$ and $\gamma_L \propto T^{-0.74}$).

The collisional deactivation rate constants from *Shved et al.* [1998] were used. In their paper the following expressions for the quenching rate constants (in cm^3s^{-1}) for collisions CO₂(01^10)-N₂, -O₂, and -O were suggested

$$k_{\text{N}_2} = 5.5 \times 10^{-17} \sqrt{T} + 6.7 \times 10^{-10} \exp(-83.8T^{-\frac{1}{3}})$$

$$k_{\text{O}_2} = 10^{-15} \exp(23.37 - 230.9T^{-\frac{1}{3}} + 564T^{-\frac{2}{3}})$$

$$k_{\text{O}} = 3 \times 10^{-12}$$

To determine the rate constants for the collisional quenching of the vibrational states higher than the first one, the harmonic law relating the rate constants for states with different degrees of excitation was used. It was also assumed that the total combined quenching rates for the second vibrational states (10^00 , 02^20 , and 02^00) are equal to $3k_{\text{N}_2}$ and $3k_{\text{O}_2}$ for collisions CO₂-N₂ and -O₂, respectively (see *Shved et al.* [1998] for details).

The value of k_{O} is one of the most important, but still not well known, factors determining the energy balance in the lower thermosphere. Laboratory measurements carried out by *Shved et al.* [1991] (for temperature range of 290-350 K) and by *Pollock et al.* [1993] (at room temperature) found the values of k_{O} to be $(1.5 \pm 0.5) \times 10^{-12} \text{ cm}^3 \text{ s}^{-1}$ and $(1.2 \pm 0.2) \times 10^{-12} \text{ cm}^3 \text{ s}^{-1}$, respectively. Analysis of satellite observations of solar radiation absorption in CO₂ infrared lines [*Lopez-Puertas et al.*, 1992] provided $k_{\text{O}} = 3.6 \times 10^{-12} \text{ cm}^3 \text{ s}^{-1}$. For our calculations we used $k_{\text{O}} = 3 \times 10^{-12} \text{ cm}^3 \text{ s}^{-1}$, the value which represents the lower limit of the satellite observations and is close to the upper limit of the laboratory experiments. This value is also supported by *Bougher et al.* [1994], who have found that Venus, Earth, and Mars simulations all agree that

$3 \times 10^{-12} \text{ cm}^3 \text{ s}^{-1}$ is the best rate to use to yield the CO₂ cooling rates required in each of the respective thermospheres.

The values of ϵ in the NLTE layer, obtained using the present method, have been recently compared with those obtained from a comprehensive solution of the CO₂ NLTE problem [Ogibalov *et al.*, 1998]. Two hundred sixty vibrational transitions associated with the 156 vibrational states of the $\nu_1\nu_2$ mode manifold for seven CO₂ isotopes were taken into consideration in that study. Nevertheless, the comparison [Ogibalov *et al.*, 1997] showed that the difference in values of ϵ obtained with their extremely comprehensive model and with the present relatively simple method is generally <10% for a wide range of input atmospheric parameters.

3. Input Atmospheric Data

The cooling rate in the 15 μm CO₂ band is quite sensitive to variations in atmospheric parameters such as temperature, [O], and [CO₂] and much less so to [N₂] and [O₂]. In order to develop and test the parameterization a set of reference calculations of cooling rate for different sets of input atmospheric parameters has been created. These sets of input parameters represent a wide variety of atmospheric conditions and include models of vertical profiles for temperature T and volume mixing ratios for CO₂ (c_{CO_2}), O (c_{O}), N₂ (c_{N_2}), and O₂ (c_{O_2}). These are discussed below.

3.1. CO₂ in the Lower Thermosphere

The CO₂ number density in the lower thermosphere is not well known. A handful of [CO₂] measurements have been conducted, mostly at midlatitudes, at different times of day and year and with different techniques. These measurements exhibit considerable variability in the reported number densities, but when reduced to the mixing ratio as a function of the dimensionless height x , the CO₂ abundance appears to be less dependent on local conditions. There are two common features observed in all CO₂ measurements: (1) nearly constant c_{CO_2} values up to $\sim x = 12-13$ ($z \approx 83-88$ km) and (2) a rapid decline in c_{CO_2} above this region.

To establish a c_{CO_2} profile in the lower thermosphere, we examined the published measurements of CO₂ conducted with the mass spectrometer technique of Offermann *et al.* [1981] and Trinks and Fricke [1978] as well as results obtained from the Atmospheric Trace Molecule Spectroscopy (ATMOS)/Spacelab 3 observations [Rinsland *et al.*, 1992]. Only the latter observations provide all the necessary information needed to calculate the $c_{\text{CO}_2}(x)$ dependence. The mass spectrometer measurements are in terms of altitude instead of pressure. To make use of these measurements, we took pressure profiles from the Mass Spectrometer and Incoherent Scatter (MSIS)-90 model [Hedin, 1991] using input parameters that were appropriate for each event. The resulting experimental $c_{\text{CO}_2}(x)$ profiles are plotted in Figure 3.

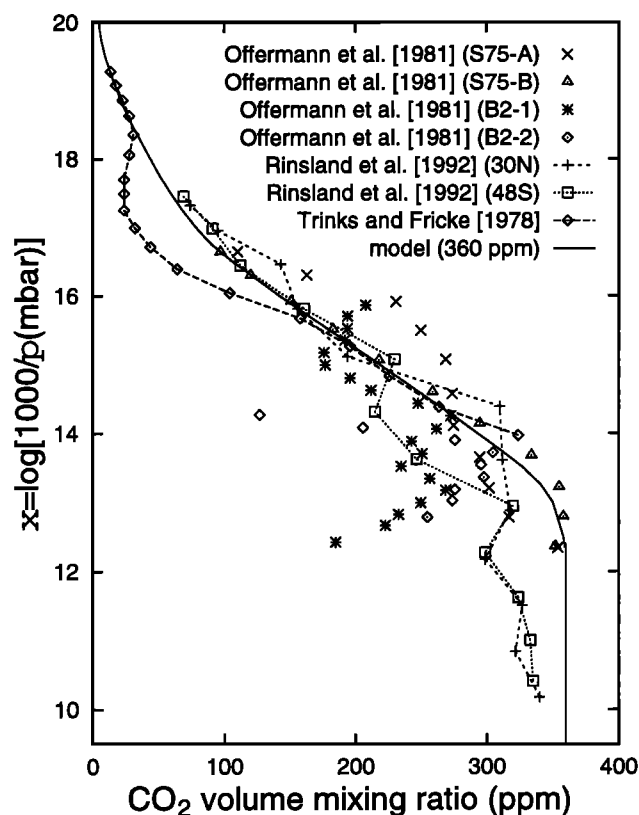


Figure 3. Model CO₂ mixing ratio profile fixed at 360 ppm below $x = 12.5$. Also shown are CO₂ mixing ratios from experiments reported in the literature (see text for details).

To construct a $c_{\text{CO}_2}(x)$ profile appropriate for current atmospheric conditions, we assumed the following:

1. Below $x = 12.5$ ($z \approx 85$ km) c_{CO_2} is assumed to be independent of height with a value of 360 ppm;
2. Between $x = 13.5$ and $x = 16.5$ ($z \approx 91-110$ km) a linear dependence on x was suggested with parameters obtained from the experimental profiles using a least squares fit. All the experimental data were weighted equally;
3. Above $x = 18.5$ ($z \approx 135$ km) the only available observation in this region [Trinks and Fricke, 1978] was used;
4. A second-order interpolation was used to merge the aforementioned intervals.

This derived c_{CO_2} profile is also presented in Figure 3.

3.2. Input Data Sets for Reference Calculation

3.2.1. Temperature and O. For a given CO₂ abundance the cooling rate in the middle and upper atmosphere is primarily dependent on temperature and O abundance. Whereas temperature along with the CO₂ abundance affects cooling rate values at all heights, O is only important in the NLTE layer above $\sim x = 13$ ($z \approx 88$ km) where the 15 μm CO₂ band source function is strongly dependent on O abundance [e.g., Fomichev *et al.*, 1996]. In our study we utilized six models of $T(x)$ and $c_{\text{O}}(x)$. These models are meant

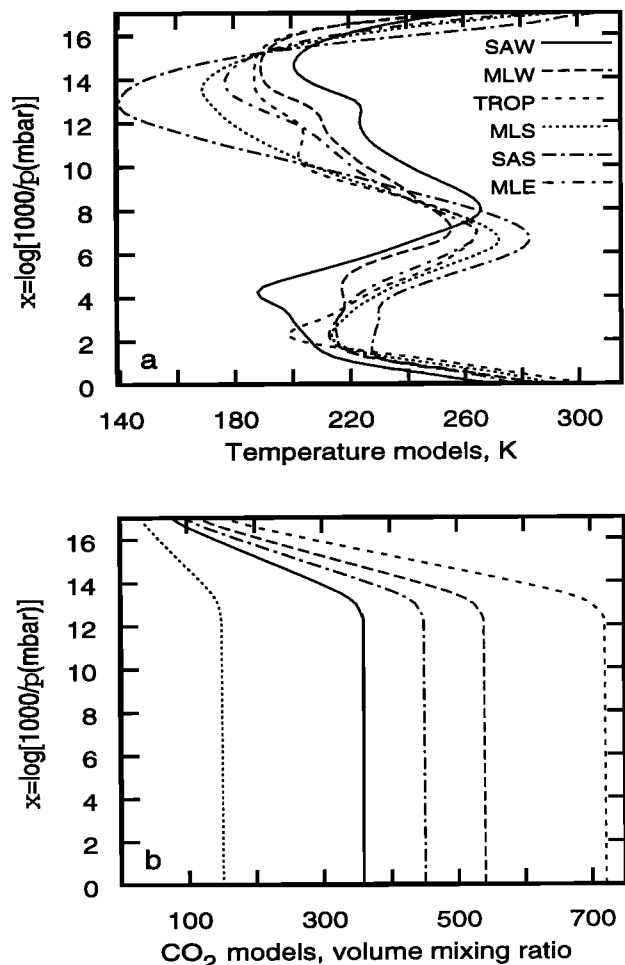


Figure 4. (a) Model temperature and (b) CO₂ mixing ratio profiles used to create and test the parameterization. Figure 4a shows temperature profiles taken from the CIRA-1986 model (see Figure 1 for notation). Figure 4b shows basic models for CO₂ mixing ratio profiles fixed at 150, 360, 540, and 720 ppm below $x = 12.5$. The CO₂ mixing ratio profile, fixed at 450 ppm below $x = 12.5$, is used to test CO₂ dependence of the parameterization.

to be a representative sample of typical climatological atmospheric conditions and include Subarctic winter (SAW) and summer (SAS), middle latitude winter (MLW), summer (MLS), and equinox (MLE), and tropics (TROP). The $T(x)$ profiles used in this study were taken from the COSPAR International Reference Atmosphere (CIRA)-86 model [Fleming et al., 1990] and are presented in Figure 4a. To construct $c_{\text{O}}(x)$ models for appropriate latitudes and seasons, [O] vertical profiles from Llewellyn et al. [1989] together with total number densities and pressure profiles from the MSIS-90 model [Hedin, 1991] were utilized.

3.2.2. CO₂. The c_{CO_2} models used in this study are shown in Figure 4b. Reference calculations for each of the six aforementioned atmospheric models were performed using four basic CO₂ mixing ratio profiles with fixed values at 150, 360, 540, and 720 ppm below $x = 12.5$ ($z \approx 85$ km). These models were created by appro-

priately scaling the 360 ppm model illustrated in Figure 3 using the ratio of the mixing ratios. In addition, an extra calculation for the three extremal atmosphere models (SAW, TROP, and SAS) assuming a c_{CO_2} value of 450 ppm was constructed. This calculation was not used in the development of the parameterization but was used to test how well the parameterization handled an arbitrary CO₂ mixing ratio.

3.2.3. O₂ and N₂. The c_{O_2} and c_{N_2} values are nearly constant up to the level $x = 13$ ($z \approx 88$ km). Above this level the dependence of cooling rate on c_{O_2} and c_{N_2} is negligible in comparison to its dependence on $c_{\text{O}}(x)$. Consequently, for all latitudes and seasons the same $c_{\text{O}_2}(x)$ and $c_{\text{N}_2}(x)$ profiles (taken from the United States Standard Atmosphere (USSA)-76 model [Chamberlain and Hunten, 1987]) were used in our calculations.

4. Method

There are two regions in the middle atmosphere where it is relatively simple to create a parameterization. The first one is the LTE region below $\sim x = 10$ ($z \approx 70$) where the cooling rate is only sensitive to variations in T and c_{CO_2} . The second region is the NLTE layer above $x = 14$ ($z \approx 93$) where the fundamental band of the ¹²C¹⁶O₂ isotope dominates the radiative cooling, and the recurrence formula of Kutepov and Fomichev [1993] can be utilized without any additional modifications. The most difficult region for creating a matrix parameterization is the transition region between $x = 10$ and $x = 14$. In this region the LTE condition starts to break down, but many of the vibrational transitions comprising the 15 μm CO₂ band still contribute significantly to the radiative cooling. Below we consider approaches used to develop the parameterization in each of these regions.

4.1. Matrix Parameterization for the LTE Layer

The parameterization for the LTE layer is based on the line-by-line calculation presented in section 2.1. It was constructed using the following five steps:

1. Using the line-by-line diffuse transmittance matrices, Curtis matrices $\mathbf{A}^{\tau,s}$ were defined for each 10 cm^{-1} interval s within 540–800 cm^{-1} for each $T(x)$ profile τ and for each CO₂ model presented in section 3.2.2. With the Curtis matrices determined the cooling rate at the grid level x_0 can be evaluated using the formula

$$\varepsilon^{\tau,s}(x_0) = \sum_j A_j^{\tau,s}(x_0) \varphi_j^{\tau,s} \quad (2)$$

where

$$\varphi_j^{\tau,s} = \exp(-h\nu_s/kT_j^{\tau}) \quad (3)$$

is the exponential part of the Planck function. The index j corresponds to the set of height levels x_j within $x = 0-14$ at an interval of 0.25, h is the Planck constant, k is the Boltzmann constant, ν_s is the frequency at the center of a 10 cm^{-1} spectral interval s , and T_j^{τ} is the

air temperature for model τ at the grid level x_j . Equation (2) provides the reference line-by-line values of the cooling rate in the LTE layer.

2. The next step was to express the temperature dependence of the Curtis matrices in the form suggested by *Fomichev and Blanchet* [1995].

Curtis matrices depend on temperature through the temperature dependence of the band strength. In turn, the total strength S_b^s of each spectral interval s can be considered as a sum of the strengths of spectral lines associated with fundamental S_0^s , first hot S_1^s , and second hot S_2^s vibrational transitions. Taking into consideration that the strength of the fundamental bands depends slightly on temperature, whereas strength of the hot bands depends exponentially on the temperature, we divided the elements of the Curtis matrices into two parts and introduced the temperature dependence as follows

$$A_j^{\tau,s}(x_0) = a_j^{\tau,s}(x_0) + b_j^{\tau,s}(x_0)\varphi_0^{\tau,s}$$

where

$$a_j^{\tau,s}(x_0) = A_j^{\tau,s}(x_0) \frac{S_0^s}{S_0^s + (S_1^s + S_2^s)\varphi_0^{\tau,s}}$$

$$b_j^{\tau,s}(x_0) = A_j^{\tau,s}(x_0) \frac{S_1^s + S_2^s}{S_0^s + (S_1^s + S_2^s)\varphi_0^{\tau,s}}$$

With the elements of the Curtis matrices defined in this manner the temperature dependence is mainly concentrated in the $\varphi_0^{\tau,s}$ terms.

3. The coefficients $a_j^{\tau,s}(x_0)$ and $b_j^{\tau,s}(x_0)$ are determined for spectral intervals of 10 cm⁻¹ within 540–800 cm⁻¹. We combined these coefficients in order to obtain coefficients for the whole 15 μ m CO₂ band.

$$a_j^\tau(x_0) = \sum_s a_j^{\tau,s}(x_0)\varphi_j^{\tau,s}/\varphi_j^\tau$$

$$b_j^\tau(x_0) = \sum_s b_j^{\tau,s}(x_0)\varphi_j^{\tau,s}\varphi_0^{\tau,s}/(\varphi_j^\tau\varphi_0^\tau)$$

where φ_j^τ is determined from (2) for the frequency of the 01¹0–00⁰0 transition of the ¹²C¹⁶O₂ isotope (i.e., $\nu = 667.3799$ cm⁻¹).

4. The coefficients $a_j^\tau(x_0)$ and $b_j^\tau(x_0)$ are still different for different temperature models τ . The final step is to introduce temperature independent coefficients by combining the coefficients $a_j^\tau(x_0)$ and $b_j^\tau(x_0)$:

$$a_j(x_0) = \sum_\tau \xi^\tau a_j^\tau(x_0) \quad b_j(x_0) = \sum_\tau \xi^\tau b_j^\tau(x_0)$$

The weights ξ^τ ($\sum_\tau \xi^\tau = 1$) are determined by minimizing the function

$$\Delta(\xi^\tau) = \sum_\tau \eta^\tau \{ \varepsilon_\tau^\tau(x_0) - \sum_{\tau'} \xi^{\tau'} \sum_j [a_j^{\tau'}(x_0) + b_j^{\tau'}(x_0)\varphi_0^{\tau'}] \varphi_j^\tau \}^2$$

in a least mean squares sense. Here ε_τ^τ is the refer-

ence line-by-line cooling rate and η^τ ($\sum_\tau \eta^\tau = 1$) are the fractions of the area on the globe which can be described by a certain temperature model τ . In this study we supposed η^τ to be equal to 0.05, 0.1, 0.4, and 0.3 for Subarctic (winter and summer), midlatitude (winter and summer), tropical, and equinox temperature profiles (Figure 4a), respectively. With the new coefficients the parameterization formula for the 15 μ m CO₂ band radiative cooling in the LTE layer is transformed to the form

$$\varepsilon(x_0) = \sum_j [a_j(x_0) + b_j(x_0)\varphi_0^\tau] \varphi_j^\tau \quad (4)$$

5. The 15 μ m CO₂ band radiative cooling in the LTE layer depends on both temperature and c_{CO_2} . With (4) we have expressed the temperature dependence in an explicit form. The CO₂ dependence is present in the parameterization coefficients $a_j(x_0)$ and $b_j(x_0)$ in both explicit and implicit forms and can be expressed as $c_{\text{CO}_2}(x_0) \times \mathcal{F}(c_{\text{CO}_2})$, where $\mathcal{F}(c_{\text{CO}_2})$ is some combination of the second-order exponential integrals. We created four sets of the parameterization coefficients for the basic CO₂ models of 150, 360, 540, and 720 ppm (Figure 4b). To obtain the matrix parameterization for arbitrary CO₂ concentration, linear interpolation of the values $\log[a_j(x_0)/c_{\text{CO}_2}(x_0)]$ and $\log[b_j(x_0)/c_{\text{CO}_2}(x_0)]$ is recommended.

To calculate values of $\varepsilon(x_0)$ by (4), the parameterization coefficients and air temperature should be prescribed on a uniform height grid with a step of $\Delta x = 0.25$. We call this the full grid matrix parameterization. Employing the method of matrix transformation suggested by *Akmaev and Fomichev* [1992], the full grid matrix parameterization can be adopted to an arbitrary vertical coordinate grid. In our study we used this method in order to optimize the parameterization by minimizing the number of levels which contribute to the cooling rate at a given level as well as the number of parameterization coefficients. With the optimized vertical grid, only eight levels (Table 1) need to be considered to account for the internal heat exchange in the LTE region of the atmosphere. As will be shown in section 5, the accuracy of the parameterization with the optimized vertical grid is only slightly different than that with the full vertical grid.

Table 1. Dimensionless Height Steps Δx_j , Which Determine the Grid Points x_j Used for Calculation of $\varepsilon(x_0)$

j	Δx_j
-5	-6.25
-4	-3.00
-3	-1.75
-2	-0.75
-1	-0.25
0	0.00
1	0.25
2	0.75
3	1.50

4.2. Recurrence Formula for NLTE Layer

The second region where it is relatively simple to create a parameterization is the NLTE layer above $x \approx 14$ [$z \approx 93$ km]. Two assumptions can be made in this region which considerably simplify cooling rate calculations. These are (1) the fundamental band of the $^{12}\text{C}^{16}\text{O}_2$ molecule dominates the radiative cooling rate so that the contributions of other vibrational transitions can be omitted and (2) since the $15\ \mu\text{m}$ CO₂ band is optically thin above $x \approx 14$ the radiative heat exchange between a given atmospheric level in this region and the atmosphere above this level can be neglected. With these assumptions the recurrence formula suggested by *Kutevov and Fomichev* [1993] can be utilized to calculate the cooling rate in the $15\ \mu\text{m}$ CO₂ band. This formula relates the value of the cooling rate in the fundamental band of the $^{12}\text{C}^{16}\text{O}_2$ molecule at a given level in the atmosphere with the value at the neighboring lower level. Starting from some lower boundary level, the cooling rate can be calculated moving upward from one height level to another. In our parameterization the value of ε at $x_0 = 13.75$ is used as a lower boundary condition.

Under NLTE conditions the $15\ \mu\text{m}$ CO₂ band cooling rate depends not only on temperature and CO₂ concentration but also on values of c_{O} , c_{O_2} , c_{N_2} , and on the quenching rate constants. The recurrence formula contains the explicit dependence of ε on all these parameters, except the CO₂ concentration. The cooling rate $\varepsilon(x_0)$ depends on the CO₂ concentration both explicitly and implicitly. First, it is proportional to the value c_{CO_2} at level x_0 , and second, it depends on the total CO₂ column amount u above level x_0 through the escape function $L(u)$. To account for the implicit dependence of ε on CO₂ concentration, values of L were calculated as a function of u , and $\log L$ was linearly interpolated over u .

Above $x \approx 16.5$ the $15\ \mu\text{m}$ CO₂ band is so optically thin that $L(u) \approx 1$ for any CO₂ model, thus it is not necessary to take into account the internal heat exchange within this region of the atmosphere to calculate the value ε . Taking this fact into consideration, we expressed the recurrence formula as a two-term formula with the first term providing cooling-to-space from a given level x_0 , and the second term describing the radiative heat exchange between level x_0 and the atmosphere below $x = 16.5$. In this two-term formula the dependence of ε on all input parameters is given in explicit form.

4.3. Transition Region

The most complicated region to parameterize the $15\ \mu\text{m}$ CO₂ band cooling is the transition region between $\sim x = 10$ – 14 ($z \approx 70$ – 93 km). NLTE effects must be taken into consideration in this region, but neither the radiative heat exchange with the overlying atmosphere nor the contribution of bands other than the fundamental band can be neglected.

Figure 5 illustrates the conditions in the transition region (see *Fomichev et al.*, [1996] for details). For il-

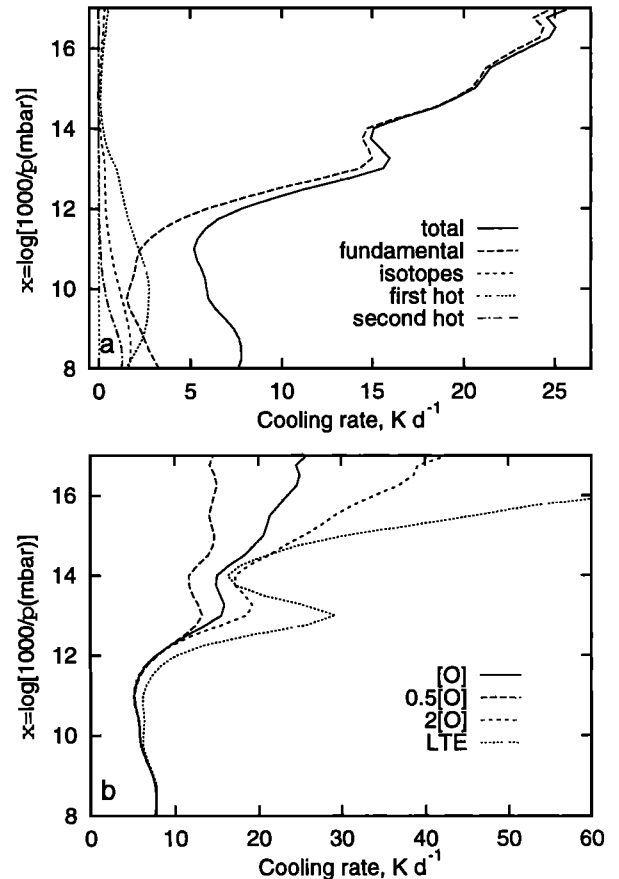


Figure 5. The $15\ \mu\text{m}$ CO₂ band cooling rate in the non-LTE (NLTE) layer for June at 70°S . (a) Contributions of different transitions to the radiative cooling rate: total, the total sum for all transitions; fundamental, the 01^10 - 00^00 transition of the $^{12}\text{C}^{16}\text{O}_2$ molecule; isotopes, the sum of the 01^10 - 00^00 transitions of the $^{13}\text{C}^{16}\text{O}_2$, $^{12}\text{C}^{16}\text{O}^{18}\text{O}$, and $^{12}\text{C}^{16}\text{O}^{17}\text{O}$ molecules; first hot, the $2\nu_2$ - ν_2 transitions of the $^{12}\text{C}^{16}\text{O}_2$ molecule; and second hot, the $3\nu_2$ - $2\nu_2$ transitions of the $^{12}\text{C}^{16}\text{O}_2$ molecule. (b) NLTE and LTE cooling rates: [O], NLTE cooling rate for input parameters appropriated to June, 70°S ; 0.5[O] and 2[O], the same but for the halved and doubled atomic oxygen abundance, respectively; and LTE, cooling rate in the case of LTE.

lustrative purposes we selected the case of the Subarctic winter where all the features discussed below are most prominent. As can be seen from Figure 5a, bands other than the fundamental band contribute substantially to the radiative cooling up to $\sim x = 14$. Moreover, the contribution of the first hot band to the total cooling between $x = 9$ and $x = 11$ is larger than that of the fundamental band. Figure 5b shows cooling rates calculated for different c_{O} models and LTE conditions. The effects of NLTE conditions start to influence the cooling rate above $x \approx 10$. On the other hand, below $x \approx 12.5$ variations in c_{O} do not significantly affect the radiative cooling.

Taking these facts into consideration, we divided the transition region into two layers. Between $x = 10$ and $x = 12.5$ ($z \approx 70$ and $z \approx 85$ km), where there is no sig-

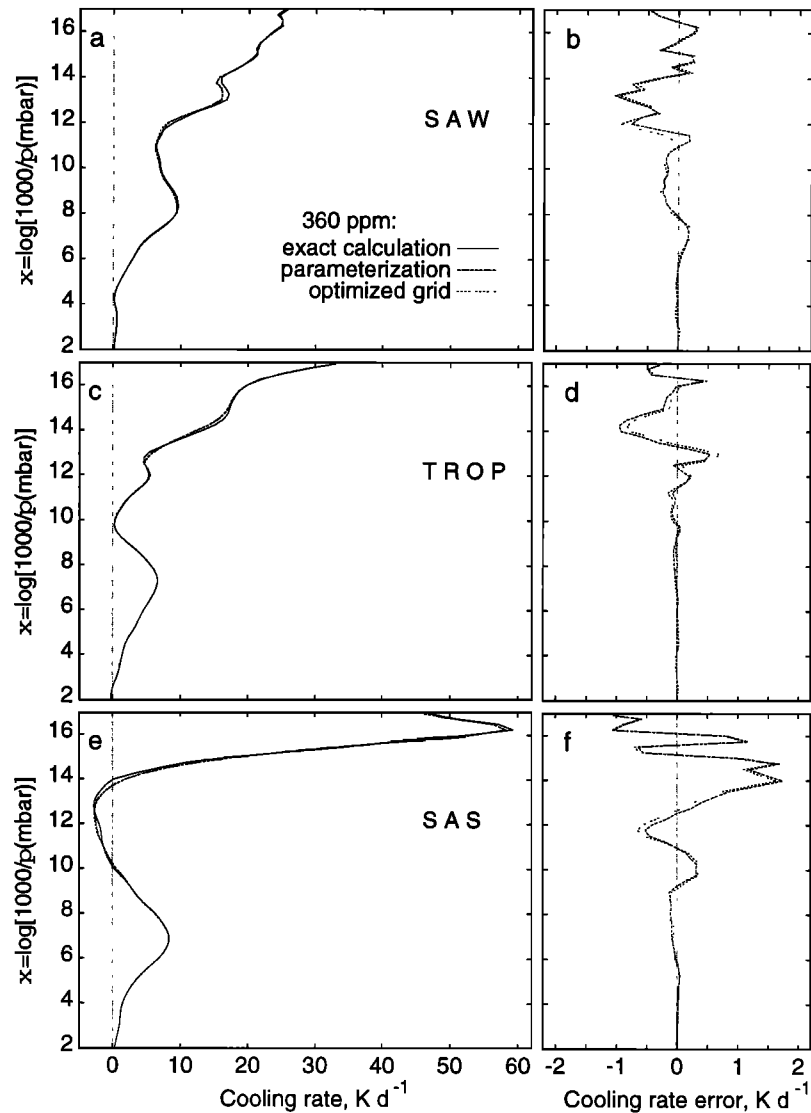


Figure 6. (a), (c), (e) Cooling rates and (b), (d), (f) cooling rate errors of the parameterization for CO₂ model 360 ppm (see Figure 4b) and for Subarctic winter (Figures 6a and 6b), tropics (Figures 6c and 6d), and Subarctic summer (Figures 6e and 6f): exact calculation, calculation made with the reference method; parameterization, calculation made with the present parameterization using a constant height step $\Delta x = 0.25$ to account for the internal atmospheric heat exchange; and optimized grid, calculation made with the present parameterization using the optimized vertical grid (Table 1) to account for the internal atmospheric heat exchange (see text for details).

nificant influence of atomic oxygen on the cooling rate and where c_{O_2} and c_{N_2} are nearly constant, the matrix approach (equation (4)) was used with the parameterization coefficients corrected in such a way as to include NLTE effects. Between $x = 12.5$ and $x = 14$ ($z \approx 85$ and $z \approx 93$ km) the recurrence formula of *Kutepov and Fomichev* [1993] was used with correction parameters introduced to correct the escape function in such a way as to account for both the radiative heat exchange with the overlying atmosphere and the contribution of bands other than the fundamental band. Both the parameterization coefficients for the layer $x = 10$ – 12.5 and correction parameters for the layer $x = 12.5$ – 14 were obtained by minimizing the error of the parameterization using

least mean squares methods similar to the one described in section 4.1. Sets of the parameterization coefficients and correction parameters were created for four basic CO₂ models of 150, 360, 540, and 720 ppm (Figure 4b), and a linear interpolation of the logarithms of its values was used in order to obtain the parameterization for an arbitrary CO₂ concentration.

5. Accuracy of the Parameterization

In this section the cooling rates of the $15 \mu\text{m}$ CO₂ band generated by the parameterization are compared to results obtained by the reference method (section 2). To verify the parameterization, the comparison has

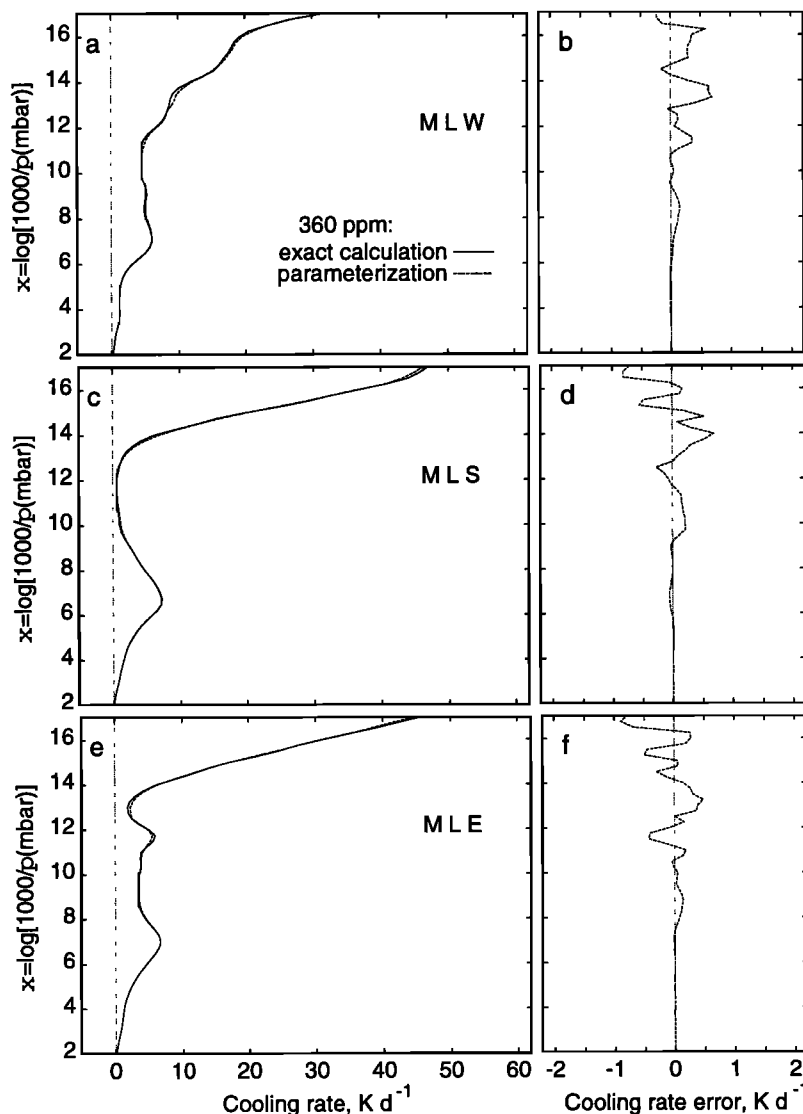


Figure 7. The same as in Figure 6 but for (a) and (b) midlatitude winter, (c) and (d) midlatitude summer, and (e) and (f) midlatitude equinox.

been carried out for the wide range of input atmospheric parameters (temperature and atmospheric composition) described in section 3 and illustrated in Figure 4. Although the parameterization, as implemented, is applicable in the middle and upper atmosphere, its accuracy was investigated only in the region between $x = 2$ and $x = 17$, where reference cooling rate calculations were available.

Figure 6 compares cooling rates obtained for the 360 ppm CO₂ model and for extremal conditions of the Subarctic winter and summer and the tropics. Two versions of the parameterization, full and optimized grids, have been tested and showed almost the same accuracy throughout the domain.

As can be seen from Figure 6, the present parameterization provides a reasonable approximation for the cooling rates for a range of input atmospheric parameters and the height region under consideration. The difference between the cooling rates obtained with the

reference method and the parameterization does not exceed 0.15 and 0.3 K d⁻¹ below $x = 7$ and $x = 11$, respectively. This is much better than the accuracy of the parameterizations by *Fomichev et al.* [1993] and *Fomichev and Blanchet* [1995] where the cooling rates were underestimated by 0.5–0.8 K d⁻¹ near the stratopause. The maximum error for the present parameterization occurs in the transition region between $x = 12$ and $x = 14.5$, where it reaches 1.6 K d⁻¹ for the Subarctic summer and ~ 1 K d⁻¹ for the tropics and Subarctic winter conditions. The parameterization of *Fomichev et al.* [1993] has a similar accuracy in the transition region, and it appears unlikely that the accuracy of the parameterization in this region can be improved within the context of the matrix-recurrence relationship approach used here. On the other hand, this approach provides a highly efficient computational parameterization of the cooling rate. It should also be noted that the maximum error occurs in the narrow Subarctic region during the sum-

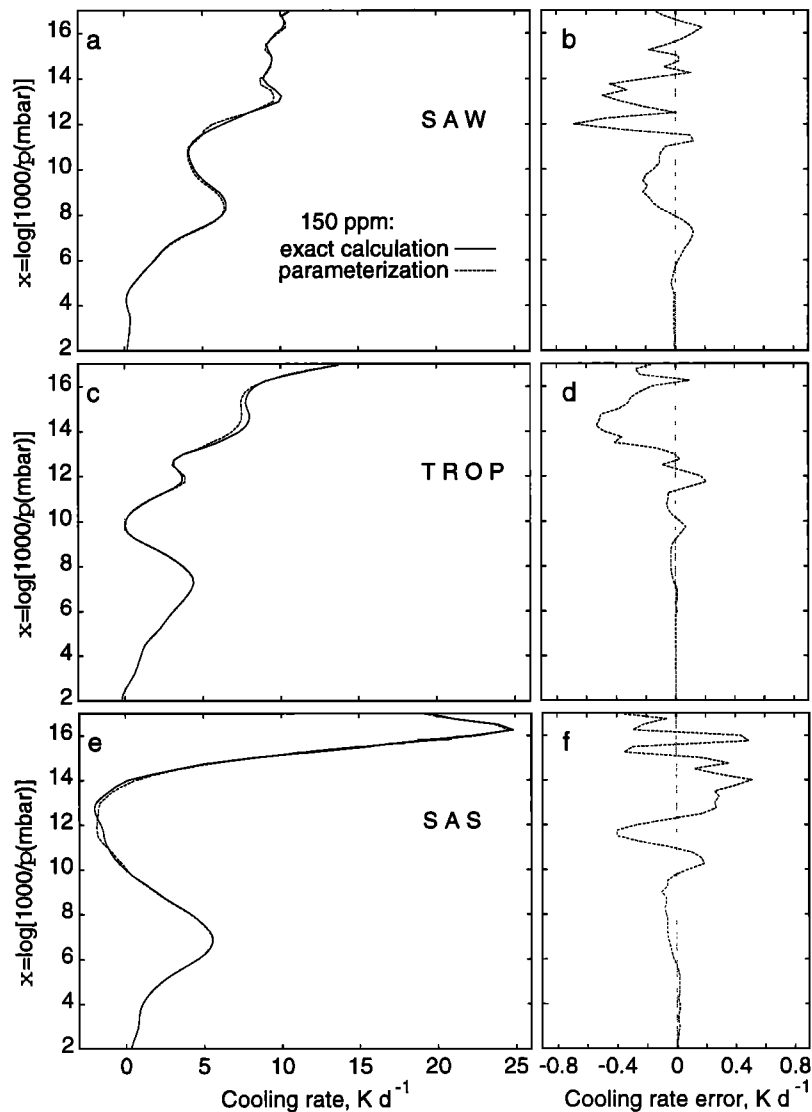


Figure 8. The same as in Figure 6 but for CO₂ model 150 ppm (see Figure 4b).

mer season, and errors are much less for other regions and seasons. In the NLTE layer above $x \approx 14.5$ the accuracy of the present parameterization is better than 1 K d^{-1} (or $\sim 5\%$) for a range of input atmospheric parameters.

The parameterization works much better in the mid-latitude regions, where the error does not exceed $\sim 0.5 \text{ K d}^{-1}$ for most of the domain (Figure 7). Error curves in Figure 7 look like noise, especially in the upper part of the domain, where the error is $\sim 0.5\text{--}0.7 \text{ K d}^{-1}$ or $< 2\%$. Taking into consideration that the accuracy of the parameterization in the midlatitude regions is much better than that in the case of the extreme Subarctic and tropics conditions, only results for these extremal conditions are presented hereafter.

Figures 8 and 9 show the comparison of the reference and parameterization cooling rates for the 150 and 720 ppm CO₂ models, respectively. For the 150 ppm CO₂ model the parameterization provides cooling rates with errors $< 0.5 \text{ K d}^{-1}$ throughout all the domain. The

error curves for the 720 ppm CO₂ model are similar to those shown in Figure 6. The deviation from the reference results is within 0.5 K d^{-1} in the height region below $\sim x = 11$ for any input atmospheric parameters and has a maximum in the transition region where the error reaches $\sim 5 \text{ K d}^{-1}$ for the Subarctic summer and $\sim 2 \text{ K d}^{-1}$ for the tropics and Subarctic winter atmospheres.

One of the main features required from the $15 \mu\text{m}$ CO₂ radiative cooling parameterization is a proper response to variations in c_{O} occurring in the lower thermosphere. Figure 10 presents the results obtained for doubled and halved c_{O} . As can be seen from Figure 10, above $x = 12.5$, where we use the recurrence formula, the parameterization responds appropriately to variations in atomic oxygen concentration. The difference in cooling rates between the reference method and parameterization obtained with the halved c_{O} does not exceed 1 K d^{-1} throughout all the domain for any temperature profiles, whereas the error obtained with the doubled c_{O}

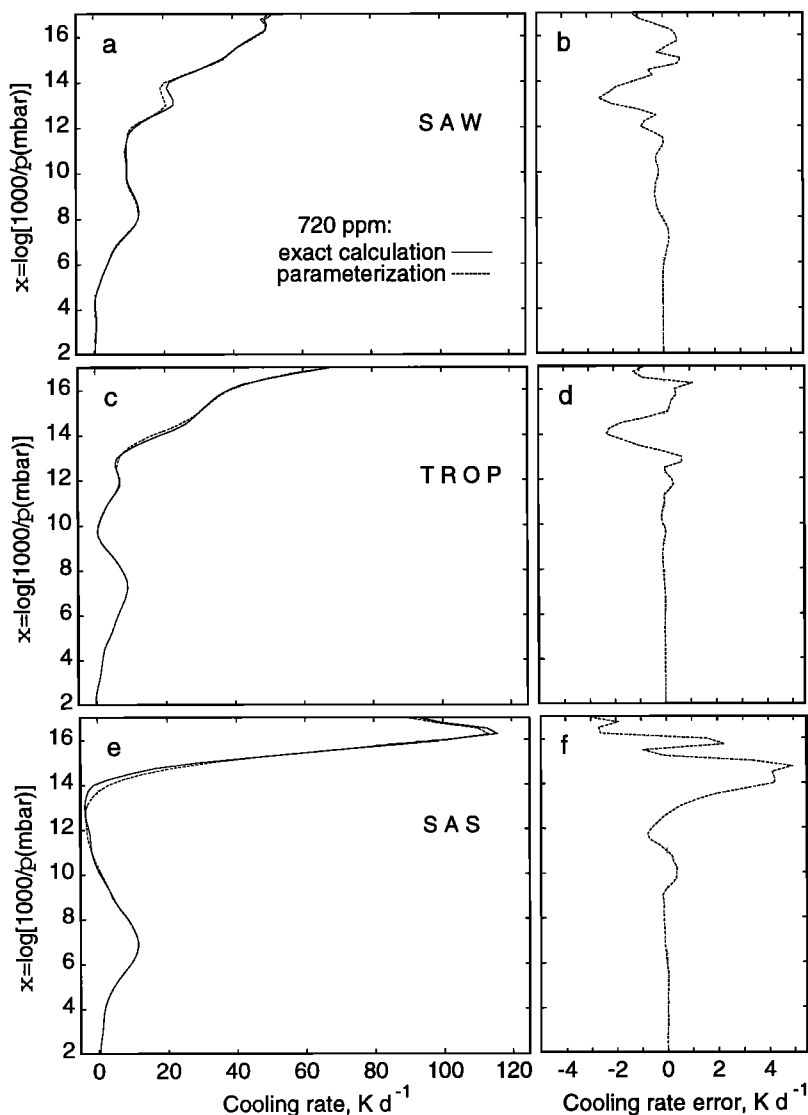


Figure 9. The same as in Figure 6 but for CO₂ model 720 ppm (see Figure 4b).

reaches 4, 2, and 1 K d^{-1} for Subarctic summer, Subarctic winter, and tropics, respectively. The error curves are generally similar to those obtained with the undisturbed c_{O} profile. It is worth noting here that since the value of ϵ is actually dependent on the product $k_{\text{O}} \times [\text{O}]$ a test for sensitivity to O variations is, at the same time, a test for sensitivity to variations of the k_{O} constant.

A final test has been carried out in order to verify the ability of the parameterization to reproduce cooling rates for CO₂ concentrations other than the basic ones. For this purpose the reference method has been applied to the 450 ppm CO₂ model (Figure 4b), and the parameterization coefficients for this CO₂ model have been obtained by interpolating the coefficients precalculated for the basic CO₂ models. Figure 11 shows the comparison of the cooling rates provided by the reference method and by the parameterization for 450 ppm CO₂ model. The results obtained with the reference method for other basic CO₂ models (150, 360, 540, and 720 ppm) are also shown in Figure 11. Variations in c_{CO_2} cause cooling rate variations which are different in

different height regions. The difference in the cooling rates associated with different CO₂ models lies within a few K d^{-1} below the mesopause and increases rapidly in the lower thermosphere where the atmosphere becomes transparent in the 15 μm CO₂ band and the cooling rate is roughly proportional to c_{CO_2} at a given height. For the 450 ppm CO₂ model the deviations between the parameterization and reference method results are generally much smaller than the differences between cooling rates for the 450 and 360 ppm (as well as for 450 and 540 ppm) CO₂ models. This deviation lies within $\sim 1 \text{ K d}^{-1}$ throughout the domain for both the Subarctic winter and tropics and for most of the domain for the Subarctic summer. The maximum error of $\sim 2.5 \text{ K d}^{-1}$ occurs in the transition region $x = 12.5$ – 14 for the Subarctic summer atmosphere. Comparing the results shown in Figure 11 with those in Figures 6 and 9, it can be concluded that the parameterization approximates the cooling rate values for arbitrary CO₂ concentrations with the same accuracy as it does for the basic CO₂ models.

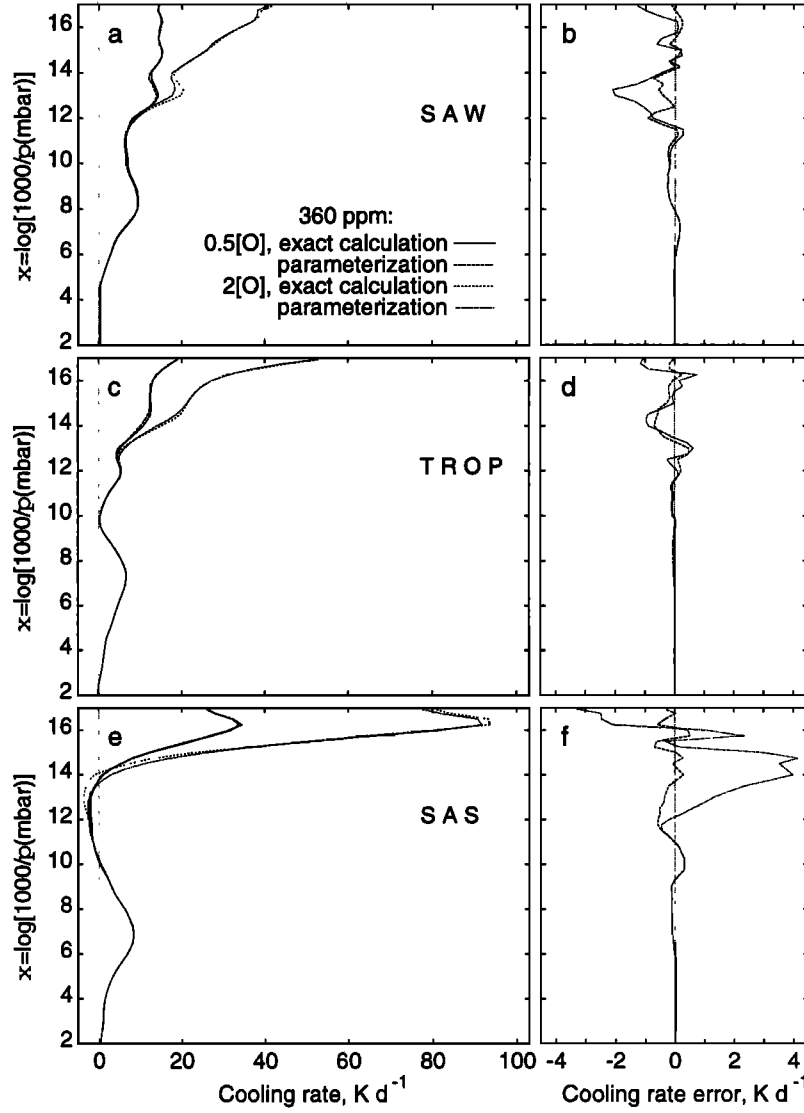


Figure 10. The same as in Figure 6 but for doubled and halved atomic oxygen abundances.

6. Parameterization Scheme

In this section the parameterization of the $15\ \mu\text{m}$ CO₂ band radiative cooling designed for the optimized height grid is presented. In order to calculate the radiative cooling rate ε all input information (air temperature T , air molecular weight μ , volume mixing ratios c_{N_2} , c_{O_2} , c_{O} , and c_{CO_2} for gases N₂, O₂, O, and CO₂) should be prescribed as a function of the dimensionless height x (equation (1)). The value c_{CO_2} should be fixed to a value between 150 and 720 ppm below $x = 12.5$ and may vary with height above this level. The values of ε provided by the parameterization are given in $\text{erg}(\text{g s})^{-1}$.

For the height $x_0 = 2\text{--}12.5$, ε is approximated by

$$\varepsilon(x_0) = \sum_{j=-5}^3 [a_j(x_0) + b_j(x_0)\varphi_0]\varphi_j \quad (5)$$

where

$$\varphi_j = \exp(-960.217/T_j) \quad (6)$$

and $T_j = T(x_j)$ is the air temperature in kelvins. The index j corresponds to the set of height levels x_j , which for every x_0 and $j = -5, -4, \dots, 2, 3$ are defined by expression $x_j = x_0 + \Delta x_j$. The intervals Δx_j are presented in Table 1 (if $x_j < 0$, $x_j = 0$ should be taken). For each given j , x_0 , and specified c_{CO_2} , the parameters $a_j(x_0)$ and $b_j(x_0)$ are obtained by interpolating over c_{CO_2} between sets of values $a_{150j}(x_0)$, $a_{360j}(x_0)$, $a_{450j}(x_0)$, and $a_{720j}(x_0)$ and $b_{150j}(x_0)$, $b_{360j}(x_0)$, $b_{450j}(x_0)$, and $b_{720j}(x_0)$, respectively (Tables 2-9). Linear interpolation of the values $\log[a_j(x_0)/c_{\text{CO}_2}(x_0)]$ and $\log[b_j(x_0)/c_{\text{CO}_2}(x_0)]$ is recommended for those sets of parameters which do not change sign. Otherwise a second-order interpolation of the parameters themselves should be used.

In the height region $x_j = 12.75\text{--}16.5$ the value ε is determined by the formula

$$\varepsilon(x_j) = \frac{2.63187 \times 10^{11} c_{\text{CO}_2,j} (1 - \lambda_j)}{\mu_j} \tilde{\varepsilon}(x_j) \quad (7)$$

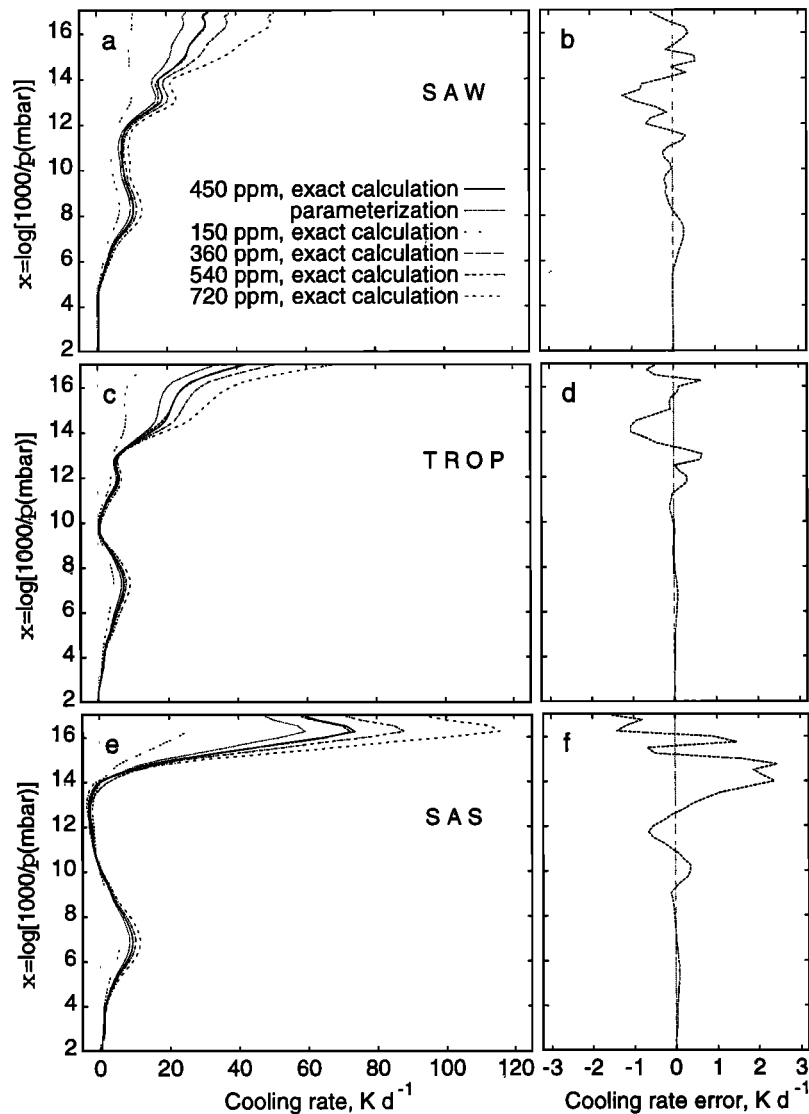


Figure 11. The same as Figure 6 but for the nonbasic CO₂ model 450 ppm (see Figure 4b). The results obtained with the reference method for the basic CO₂ models 150, 360, 540, and 720 ppm are also shown.

where

$$\lambda_j = \lambda(x_j) = 1.5988 / \{ 1.5988 + \rho_j [c_{N_2,j} (5.5 \times 10^{-17} \sqrt{T_j} + 6.7 \times 10^{-10} \exp(-83.8 T_j^{-\frac{1}{3}})) + c_{O_2,j} (10^{-15} \exp(23.37 - 230.9 T_j^{-\frac{1}{3}} + 564 T_j^{-\frac{2}{3}})) + c_{O,j} k_O] \} \quad (8)$$

$\mu_j = \mu(x_j)$ is the mean molecular weight (in g mol^{-1}), and $\rho_j = \rho(x_j)$ is the number density (in cm^{-3}) of the background atmosphere; $c_{CO_2,j} = c_{CO_2}(x_j)$, $c_{N_2,j} = c_{N_2}(x_j)$, $c_{O_2,j} = c_{O_2}(x_j)$, and $c_{O,j} = c_O(x_j)$; k_O (in $\text{cm}^3 \text{s}^{-1}$) is the rate coefficient for the collisional deactivation $\text{CO}_2(01^1_0)\text{-O}$. The value of $\tilde{\epsilon}(x_j)$ is determined by the recurrence formula

$$[1 - \lambda_j(1 - D_j)]\tilde{\epsilon}(x_j) = [1 - \lambda_{j-1}(1 - D_{j-1})]\tilde{\epsilon}(x_{j-1}) + D_{j-1}\varphi_{j-1} - D_j\varphi_j \quad (9)$$

with the boundary condition at $x = 12.5$,

$$\tilde{\epsilon}(12.5) = 1.10036 \times 10^{-10} \epsilon(12.5) / \{ c_{CO_2}(12.5)[1 - \lambda(12.5)] \} \quad (10)$$

where $\epsilon(12.5)$ is determined from (5). In (9)

$$\begin{aligned} D_j &= \frac{1}{4}(d_{j-1} + 3d_j) \\ D_{j-1} &= \frac{1}{4}(3d_{j-1} + d_j) \end{aligned} \quad (11)$$

where

$$d_j = \begin{cases} \alpha(u, x_j)L(u) & 12.5 \leq x_j \leq 13.75 \\ L(u) & x_j \geq 14.00 \end{cases} \quad (12)$$

Table 2. The Values $10^{-1} \times a150_j(x_0)$ for $-5 \leq j \leq 3$ Calculated With a Step $\Delta x_0 = 0.25$ in the Dimensionless Height Range $2 \leq x_0 \leq 12.5$

x_0	j								
	-5	-4	-3	-2	-1	0	1	2	3
2.00	2.50	0.00	9.41	247.65	324.67	-1109.0	40.70	210.62	62.00
2.25	3.15	0.00	15.66	318.86	305.56	-1256.0	21.71	221.57	77.18
2.50	3.62	0.00	25.39	388.67	285.25	-1400.9	-0.39	225.76	91.03
2.75	3.95	0.00	40.54	446.74	261.99	-1520.3	-20.23	224.54	101.23
3.00	4.39	0.00	63.52	494.90	238.73	-1628.2	-40.15	223.34	109.83
3.25	1.49	5.21	88.19	540.55	213.11	-1730.5	-57.15	224.65	117.36
3.50	1.88	8.24	111.80	579.43	189.08	-1824.7	-71.04	230.30	123.35
3.75	2.30	12.96	130.44	613.69	168.79	-1912.1	-84.78	240.19	127.64
4.00	2.71	19.75	144.27	643.90	149.97	-1989.6	-98.53	254.05	129.46
4.25	3.01	28.48	156.05	668.46	134.69	-2058.2	-111.15	270.10	129.51
4.50	3.31	38.72	167.72	689.08	126.66	-2129.9	-123.33	290.02	129.22
4.75	3.68	50.03	181.86	708.44	123.77	-2214.3	-139.97	313.84	130.38
5.00	4.10	62.58	197.91	730.78	118.88	-2313.8	-158.39	341.94	133.43
5.25	4.55	75.18	212.09	758.51	112.25	-2422.1	-180.76	373.50	137.78
5.50	5.06	88.36	223.46	792.75	100.78	-2529.0	-206.53	405.77	142.64
5.75	5.63	102.56	232.51	832.40	85.71	-2637.6	-234.40	438.96	148.27
6.00	6.26	117.99	241.92	875.37	71.11	-2753.2	-262.84	474.08	154.89
6.25	6.95	135.13	253.85	920.24	59.85	-2883.7	-290.66	512.30	163.15
6.50	9.87	146.43	271.98	967.27	56.54	-3032.4	-317.08	553.86	174.11
6.75	14.21	155.87	294.12	1018.3	62.96	-3207.4	-342.38	598.32	189.06
7.00	20.88	163.15	319.41	1075.7	80.53	-3414.1	-366.62	643.68	209.64
7.25	30.51	169.87	346.35	1142.9	107.47	-3658.5	-388.43	689.32	238.07
7.50	43.09	176.34	376.50	1225.3	144.49	-3948.7	-409.49	735.21	276.04
7.75	56.23	185.45	409.22	1328.6	186.55	-4296.9	-431.41	777.26	331.37
8.00	65.59	197.89	441.92	1447.3	227.32	-4675.8	-451.19	810.60	400.69
8.25	71.49	213.91	475.55	1579.2	263.29	-5078.4	-469.36	837.81	479.06
8.50	75.92	233.06	513.21	1723.6	297.79	-5517.9	-488.28	871.36	551.38
8.75	81.06	254.62	557.25	1876.1	333.68	-6000.7	-507.88	919.50	610.26
9.00	86.94	276.84	610.37	2016.5	377.11	-6479.2	-528.66	990.49	617.27
9.25	94.29	301.23	668.75	2122.5	442.66	-6934.1	-553.92	1104.0	552.20
9.50	101.89	324.97	723.00	2069.8	513.05	-7119.1	-574.78	1251.0	355.34
9.75	114.49	370.84	746.30	1949.5	555.11	-7381.9	-549.97	1497.2	231.95
10.00	129.99	433.25	747.55	1633.8	517.50	-7516.6	-447.53	1753.0	245.55
10.25	145.12	503.31	702.24	1518.0	326.75	-7813.4	-303.85	2043.0	274.39
10.50	158.38	576.55	600.92	1419.9	509.35	-8093.8	-318.73	2139.7	238.26
10.75	168.05	667.68	429.56	1481.1	843.27	-8625.6	-419.12	2291.9	148.85
11.00	177.01	778.03	343.48	1856.9	1368.7	-10164	-614.59	2701.7	143.67
11.25	210.81	985.59	333.85	2545.3	1916.3	-13508	-791.00	4037.1	316.37
11.50	251.17	1204.3	298.37	3052.5	2119.0	-16547	-1036.1	5575.3	638.50
11.75	272.71	1313.1	140.05	3177.7	1826.1	-17548	-1289.1	6474.4	990.29
12.00	248.17	1254.9	125.21	3250.6	1590.1	-16344	-1708.0	5950.6	798.04
12.25	204.50	1140.3	388.51	3709.8	1321.5	-15453	-2125.7	5225.6	547.05
12.50	176.09	1178.2	733.94	3600.3	572.92	-14489	-2151.8	4741.9	207.65

$L(u)$ is the escape function which depends only on the total CO₂ column amount u above a given level x_j . This dependence is presented in Table 10. In order to calculate $L(u)$ for a given c_{CO_2} profile it is recommended that a linear interpolation of logarithm of $L(u)$ be used. Since $L(u)$ depends only on u the coefficients d_j for the region $x_j \geq 14.00$ can be calculated on an arbitrary height grid. In our calculation we have used a height grid with step $\Delta x_j = 0.25$ throughout the domain. To determine the coefficients d_j in the region $12.5 \leq x_j \leq 13.75$, the parameters $\alpha(u, x_j)$ are also needed. The dependence of $\alpha(u, x_j)$ on u at levels $x_j = 12.5-13.75$ with step $\Delta x_j = 0.25$ is presented

in Table 11. To obtain the parameters $\alpha(u, x_j)$ for a user-defined c_{CO_2} profile, linear interpolation of the logarithm of $\alpha(u, x_j)$ at each level x_j is recommended.

In the region $x_j > 16.5$ the value ε can be determined by the following simple formula which provides a smooth transition to the cooling-to-space approximation and does not require any parameterization coefficients

$$\varepsilon(x_j) = \frac{2.63187 \times 10^{11} c_{\text{CO}_2, j} (1 - \lambda_j)}{\mu_j} [\Phi(16.5) - \varphi_j] \quad (13)$$

where

Table 3. The Values $10^{-3} \times b150_j(x_0)$ for $-5 \leq j \leq 3$ Calculated With a Step $\Delta x_0 = 0.25$ in the Dimensionless Height Range $2 \leq x_0 \leq 12.5$

x_0	j								
	-5	-4	-3	-2	-1	0	1	2	3
2.00	3.54	0.00	6.05	59.11	24.12	-181.03	-0.74	18.01	17.04
2.25	3.12	0.00	6.98	57.20	20.24	-171.00	-2.40	18.32	15.74
2.50	3.04	0.00	9.08	55.10	13.93	-161.06	-4.94	16.08	14.93
2.75	3.30	0.00	13.16	56.15	10.44	-167.15	-7.07	15.20	15.53
3.00	3.50	0.00	18.03	54.92	7.84	-170.25	-8.49	14.32	15.76
3.25	1.87	2.71	19.75	54.11	5.90	-171.21	-9.36	13.89	15.67
3.50	2.09	3.62	19.18	52.43	4.32	-167.30	-9.82	13.66	15.01
3.75	2.26	4.77	17.13	49.72	2.54	-158.18	-10.09	13.30	13.89
4.00	2.45	6.30	15.32	48.64	0.94	-153.18	-10.68	13.77	12.98
4.25	2.70	8.30	14.67	49.71	-0.69	-154.64	-11.83	14.87	12.64
4.50	3.01	10.34	14.76	51.02	-2.22	-157.88	-13.46	16.57	12.31
4.75	3.33	12.02	15.12	51.26	-3.76	-159.38	-15.17	18.10	11.93
5.00	3.68	13.37	15.49	50.38	-5.60	-158.54	-16.54	19.31	11.57
5.25	4.02	14.41	15.48	48.94	-7.17	-156.14	-17.64	20.52	11.21
5.50	4.32	15.29	15.28	48.66	-7.76	-156.91	-18.63	22.49	11.17
5.75	4.61	16.15	14.98	49.36	-7.94	-160.22	-19.79	25.01	11.39
6.00	4.89	17.12	14.68	50.60	-8.03	-164.87	-21.10	27.57	11.91
6.25	5.12	18.15	14.55	52.65	-8.04	-171.62	-22.73	30.24	12.70
6.50	6.95	14.81	16.72	56.07	-8.06	-181.89	-24.94	33.12	14.02
6.75	9.49	10.89	19.53	60.74	-8.20	-195.02	-27.75	35.77	15.90
7.00	13.20	6.77	22.98	66.83	-8.80	-211.16	-31.23	37.85	18.56
7.25	18.35	2.96	27.02	74.76	-10.24	-230.87	-35.39	39.28	22.03
7.50	24.24	-0.01	31.41	84.12	-12.60	-252.10	-39.94	39.90	25.64
7.75	28.90	-1.80	35.60	93.62	-16.26	-270.76	-43.92	38.27	29.58
8.00	32.23	-2.38	41.19	107.10	-21.94	-298.20	-49.13	36.91	34.89
8.25	34.90	-1.71	49.62	127.29	-29.86	-342.96	-56.74	37.39	42.35
8.50	37.69	0.27	61.73	154.70	-40.35	-407.68	-67.25	40.12	51.59
8.75	40.81	4.18	78.17	189.15	-53.54	-494.25	-80.91	45.42	62.22
9.00	43.38	10.52	99.17	226.58	-67.76	-594.81	-96.67	54.28	69.25
9.25	45.67	19.16	123.99	259.79	-80.92	-697.22	-113.91	68.93	67.84
9.50	48.15	29.65	151.97	269.05	-90.13	-768.51	-130.01	89.27	49.05
9.75	51.97	45.70	177.20	260.58	-99.25	-844.00	-142.48	119.06	35.84
10.00	57.38	67.58	198.71	214.24	-105.92	-901.96	-143.24	148.35	38.64
10.25	63.80	94.18	204.41	196.44	-130.89	-973.26	-139.77	179.13	43.02
10.50	70.64	123.95	189.16	171.95	-110.44	-1026.5	-145.44	195.45	36.84
10.75	76.84	161.72	149.09	169.11	-75.70	-1097.3	-159.36	216.62	24.06
11.00	83.23	208.19	128.35	206.77	-36.31	-1296.1	-192.72	262.88	21.98
11.25	96.16	285.62	119.66	287.49	-12.24	-1752.8	-242.63	409.70	41.32
11.50	113.57	375.96	98.65	365.98	16.10	-2296.2	-286.07	629.29	74.85
11.75	128.29	441.49	42.54	434.49	35.76	-2732.7	-317.40	852.28	122.50
12.00	124.81	433.49	33.62	486.85	73.97	-2761.9	-358.47	874.36	103.68
12.25	109.94	374.80	123.28	612.20	74.49	-2823.1	-438.41	848.03	79.80
12.50	101.38	372.76	243.76	711.93	140.92	-3324.3	-443.25	1053.2	32.31

Table 4. The Values $10^{-1} \times a360_j(x_0)$ for $-5 \leq j \leq 3$ Calculated With a Step $\Delta x_0 = 0.25$ in the Dimensionless Height Range $2 \leq x_0 \leq 12.5$

x_0	j								
	-5	-4	-3	-2	-1	0	1	2	3
2.00	1.71	0.00	8.30	258.29	449.82	-1339.3	94.33	285.60	54.67
2.25	2.29	0.00	14.18	343.15	460.65	-1574.2	79.38	323.02	75.44
2.50	2.73	0.00	23.16	434.74	471.06	-1824.3	55.67	346.88	98.49
2.75	3.08	0.00	37.25	525.47	470.45	-2057.2	31.05	354.62	120.07
3.00	3.55	0.00	59.80	613.81	457.52	-2270.0	-0.01	354.37	139.96
3.25	0.91	4.89	86.26	705.22	427.02	-2466.2	-30.60	356.40	156.87
3.50	1.29	8.06	115.35	787.22	387.61	-2639.6	-56.18	365.60	170.11
3.75	1.73	13.15	141.56	856.81	351.75	-2792.5	-82.21	382.62	179.43

Table 4. (continued)

x_0	j								
	-5	-4	-3	-2	-1	0	1	2	3
4.00	2.17	20.53	163.57	919.28	317.58	-2930.8	-108.72	406.24	184.41
4.25	2.54	29.82	183.84	971.78	287.42	-3052.3	-133.68	432.48	185.25
4.50	2.87	40.33	205.31	1015.1	267.04	-3168.2	-156.87	462.07	183.53
4.75	3.23	52.40	233.04	1054.6	254.51	-3299.4	-186.50	496.65	182.39
5.00	3.62	66.26	265.43	1092.0	237.93	-3443.0	-214.22	538.02	182.79
5.25	4.02	81.88	295.11	1131.5	225.43	-3603.7	-244.55	588.20	185.75
5.50	4.41	99.44	319.62	1181.2	215.71	-3783.8	-279.47	644.88	191.30
5.75	4.86	119.34	337.57	1236.5	203.83	-3964.9	-319.11	701.80	198.62
6.00	5.41	141.93	353.25	1299.0	192.02	-4157.7	-362.10	758.91	208.23
6.25	6.06	167.05	369.79	1366.4	181.83	-4364.3	-405.05	815.20	219.88
6.50	8.84	187.63	392.81	1442.7	179.44	-4600.0	-447.24	876.16	234.13
6.75	13.07	205.15	421.01	1525.4	189.10	-4867.8	-486.78	941.22	252.01
7.00	19.63	218.88	453.73	1613.4	214.84	-5171.8	-523.03	1008.0	275.44
7.25	29.25	229.99	490.57	1711.9	256.85	-5526.7	-555.88	1080.5	304.52
7.50	42.07	240.46	532.21	1828.7	317.24	-5948.0	-586.50	1159.0	344.22
7.75	56.57	254.71	578.02	1975.0	392.25	-6467.1	-617.21	1243.7	407.78
8.00	68.16	272.80	625.13	2147.4	471.61	-7053.4	-645.51	1325.0	500.17
8.25	75.82	295.31	673.97	2346.5	550.30	-7700.7	-673.21	1400.3	623.91
8.50	81.94	322.32	728.06	2573.8	625.92	-8419.0	-706.25	1472.4	767.81
8.75	88.34	352.81	790.13	2828.7	691.49	-9208.1	-747.00	1539.1	919.34
9.00	96.26	387.50	863.10	3054.4	745.19	-9987.3	-782.32	1589.6	1064.7
9.25	106.57	426.69	943.91	3195.0	720.98	-10632	-783.89	1655.2	1165.6
9.50	119.18	474.13	1019.2	2999.4	660.01	-10795	-712.20	1702.1	1171.5
9.75	134.48	530.49	1080.4	2815.2	300.57	-10807	-582.96	1954.5	1039.3
10.00	153.21	602.82	1118.2	2485.5	360.60	-10871	-528.56	2077.7	825.16
10.25	171.58	689.49	1092.0	2343.7	132.98	-11132	-451.35	2520.3	619.70
10.50	190.16	796.67	996.18	2052.5	428.17	-11362	-500.31	2719.4	449.84
10.75	212.44	938.28	755.90	1967.8	702.20	-12033	-491.26	3185.1	387.17
11.00	236.64	1126.5	566.93	2149.1	1126.5	-13697	-578.12	4048.6	296.47
11.25	279.13	1403.0	481.02	2605.0	1372.2	-17247	-515.46	5980.6	401.51
11.50	320.48	1685.5	384.14	3026.7	1867.9	-20901	-549.77	7771.8	590.62
11.75	345.14	1824.4	188.58	3403.1	2200.1	-23196	-613.86	8935.6	763.31
12.00	317.35	1785.8	152.39	3987.4	3014.4	-23702	-1206.4	8432.6	594.67
12.25	288.99	1722.6	360.62	5099.1	3834.6	-25185	-1927.7	8148.0	438.08
12.50	263.08	1951.0	663.21	5925.1	3521.7	-26413	-2589.6	8270.4	223.45

Table 5. The Values $10^{-3} \times b360_j(x_0)$ for $-5 \leq j \leq 3$ Calculated With a Step $\Delta x_0 = 0.25$ in the Dimensionless Height Range $2 \leq x_0 \leq 12.5$

x_0	j								
	-5	-4	-3	-2	-1	0	1	2	3
2.00	3.32	0.00	7.36	76.80	36.45	-240.80	4.55	19.81	24.31
2.25	3.24	0.00	8.93	76.99	35.83	-242.31	2.86	25.71	22.44
2.50	3.42	0.00	12.23	77.60	30.00	-242.45	-0.90	25.18	22.35
2.75	3.82	0.00	18.06	77.88	21.68	-242.76	-4.77	21.05	23.45
3.00	4.16	0.00	25.06	75.59	16.60	-243.95	-7.37	18.45	24.03
3.25	2.02	3.66	27.66	74.40	13.45	-245.00	-9.07	17.60	24.04
3.50	2.34	4.95	26.74	73.30	11.57	-242.82	-10.36	18.25	23.13
3.75	2.58	6.55	23.74	71.13	9.23	-233.76	-11.45	18.91	21.48
4.00	2.84	8.75	21.17	69.97	6.33	-226.45	-12.75	19.80	20.05
4.25	3.18	11.66	20.30	71.74	3.50	-228.45	-14.83	21.60	19.39
4.50	3.58	14.76	20.87	75.30	1.11	-237.39	-17.84	24.72	18.97
4.75	4.02	17.48	22.10	78.01	-1.34	-245.78	-21.35	28.00	18.42
5.00	4.50	19.89	23.92	80.26	-4.08	-255.31	-24.75	31.87	17.81
5.25	4.95	21.85	25.06	80.52	-6.68	-259.45	-27.55	35.28	16.94
5.50	5.40	23.72	25.32	79.67	-8.92	-259.48	-29.81	38.22	15.98
5.75	5.82	25.59	25.20	80.72	-9.50	-265.99	-31.84	42.60	15.46
6.00	6.22	27.63	24.95	82.66	-9.02	-275.96	-33.63	47.48	15.52
6.25	6.55	29.76	25.01	86.32	-7.69	-291.46	-35.70	53.08	16.18

Table 5. (continued)

x_0	j								
	-5	-4	-3	-2	-1	0	1	2	3
6.50	8.86	26.04	27.72	91.26	-5.64	-310.26	-38.08	58.97	17.41
6.75	12.12	21.47	31.22	97.93	-3.27	-333.60	-41.19	64.98	19.37
7.00	16.92	16.60	35.63	107.52	-0.52	-365.18	-45.43	71.58	22.54
7.25	23.50	12.02	40.69	120.32	2.38	-404.92	-50.82	78.74	27.04
7.50	31.01	8.23	46.12	135.78	5.09	-448.99	-57.14	85.64	32.39
7.75	36.72	5.67	50.95	151.58	6.08	-488.14	-62.94	88.31	39.59
8.00	40.35	4.51	56.89	172.53	4.40	-536.21	-70.08	89.43	50.07
8.25	43.15	4.59	65.64	202.08	-1.44	-601.97	-80.12	90.30	64.64
8.50	45.80	6.18	78.48	242.08	-12.29	-690.85	-94.00	92.02	82.65
8.75	48.93	9.73	96.79	294.38	-28.85	-809.49	-112.69	95.31	104.09
9.00	52.15	15.74	121.12	350.47	-49.63	-948.67	-134.05	99.65	127.58
9.25	55.29	25.00	152.48	404.43	-78.99	-1101.5	-155.85	109.08	149.91
9.50	58.42	37.74	189.33	413.50	-110.87	-1210.4	-169.12	114.41	164.53
9.75	62.52	56.22	234.53	427.79	-173.34	-1334.7	-181.77	149.98	161.36
10.00	67.85	80.62	279.57	392.40	-187.47	-1439.1	-198.84	174.45	138.90
10.25	74.32	112.85	313.47	382.43	-242.94	-1562.0	-220.47	232.39	115.89
10.50	81.98	155.29	325.09	318.30	-223.82	-1648.5	-247.82	266.96	90.61
10.75	91.46	211.30	282.60	282.33	-209.94	-1762.3	-267.61	324.15	79.59
11.00	101.84	289.12	242.85	287.82	-192.63	-2008.8	-308.16	430.60	62.82
11.25	118.06	402.23	225.17	339.73	-230.78	-2537.2	-357.16	652.88	77.64
11.50	135.86	526.31	189.82	397.60	-218.83	-3139.7	-404.67	888.36	102.55
11.75	151.33	615.62	107.83	482.41	-163.62	-3684.4	-413.72	1111.3	122.12
12.00	151.95	650.82	72.54	636.88	53.88	-4160.0	-453.47	1209.3	92.24
12.25	143.36	616.71	124.23	815.56	139.19	-4298.9	-567.67	1143.5	69.84
12.50	130.71	655.14	197.99	885.04	90.99	-4228.0	-614.82	1099.6	30.36

Table 6. The Values $10^{-1} \times a540_j(x_0)$ for $-5 \leq j \leq 3$ Calculated With a Step $\Delta x_0 = 0.25$ in the Dimensionless Height Range $2 \leq x_0 \leq 12.5$

x_0	j								
	-5	-4	-3	-2	-1	0	1	2	3
2.00	1.40	0.00	8.41	270.00	498.55	-1442.8	119.32	311.12	52.29
2.25	1.84	0.00	13.81	355.08	524.98	-1703.6	110.96	364.61	71.57
2.50	2.29	0.00	22.67	453.27	556.70	-2007.2	90.70	406.62	96.77
2.75	2.68	0.00	36.64	556.19	580.94	-2312.6	67.68	427.55	123.65
3.00	3.13	0.00	58.73	661.92	586.20	-2599.0	33.72	432.06	150.84
3.25	0.64	4.68	85.36	778.21	564.76	-2867.4	-3.24	435.42	175.54
3.50	0.96	7.89	115.48	887.91	523.30	-3102.5	-35.40	447.39	194.80
3.75	1.36	13.07	143.91	980.97	480.32	-3299.5	-68.66	469.60	207.77
4.00	1.77	20.67	168.61	1064.1	437.93	-3475.1	-102.92	500.45	214.96
4.25	2.14	30.07	192.10	1136.6	399.95	-3633.5	-135.71	534.48	217.01
4.50	2.49	40.59	218.13	1198.8	373.02	-3785.7	-167.00	571.83	215.33
4.75	2.83	52.18	253.05	1255.0	353.59	-3948.8	-207.23	612.38	213.32
5.00	3.22	66.57	295.83	1308.0	326.13	-4126.4	-244.06	661.23	211.93
5.25	3.61	83.15	336.14	1357.8	305.08	-4316.7	-280.85	720.30	213.01
5.50	4.03	102.97	370.22	1417.1	291.28	-4533.6	-321.04	789.46	217.76
5.75	4.49	125.99	396.15	1483.0	280.30	-4762.5	-366.41	862.25	225.58
6.00	5.00	152.24	417.57	1555.7	272.04	-5004.4	-416.90	935.69	236.18
6.25	5.64	182.14	438.50	1635.4	265.60	-5264.3	-469.17	1007.3	249.79
6.50	8.31	207.90	464.27	1725.4	266.78	-5550.1	-521.01	1080.9	266.17
6.75	12.39	230.45	495.15	1826.2	280.40	-5873.8	-570.19	1157.9	286.80
7.00	18.91	248.70	531.35	1935.7	311.10	-6241.9	-615.62	1237.1	313.42
7.25	28.40	262.77	573.04	2056.4	360.12	-6664.7	-655.63	1321.2	345.31
7.50	41.26	276.04	620.57	2195.9	431.64	-7162.3	-691.63	1412.9	387.11
7.75	55.91	293.04	673.24	2366.1	522.76	-7769.7	-725.78	1514.8	451.44
8.00	67.74	313.84	727.90	2564.7	622.56	-8457.8	-755.73	1620.6	544.99
8.25	76.10	339.36	785.72	2795.1	727.29	-9231.2	-784.60	1730.5	674.68
8.50	82.15	368.97	849.10	3056.5	837.12	-10096	-817.88	1842.6	833.35
8.75	89.73	403.71	921.79	3354.1	942.43	-11068	-862.95	1953.9	1019.4

Table 6. (continued)

x_0	j								
	-5	-4	-3	-2	-1	0	1	2	3
9.00	98.65	443.10	1005.1	3620.2	1034.1	-12033	-904.65	2032.3	1217.0
9.25	110.10	488.98	1097.9	3805.1	1018.3	-12865	-916.89	2114.1	1373.9
9.50	125.23	545.07	1184.5	3605.6	926.41	-13103	-857.02	2146.5	1403.2
9.75	142.90	614.93	1263.0	3466.0	461.13	-13253	-769.23	2538.5	1181.4
10.00	163.93	696.03	1304.5	3129.2	502.50	-13241	-802.18	2724.8	817.99
10.25	184.22	791.25	1285.0	2991.9	165.39	-13374	-755.23	3206.7	546.50
10.50	205.56	911.98	1195.2	2622.9	540.64	-13513	-859.19	3380.5	339.09
10.75	231.95	1076.5	942.32	2468.0	782.82	-14260	-817.16	3931.4	327.46
11.00	267.41	1305.6	736.83	2590.1	1185.3	-16172	-866.79	4935.8	312.83
11.25	312.74	1619.0	661.71	2985.2	1399.6	-20033	-716.56	7058.6	500.72
11.50	353.42	1935.7	565.59	3361.1	1782.8	-23702	-622.84	8816.3	731.70
11.75	378.34	2096.5	325.88	3701.0	2118.9	-25903	-586.21	9855.4	862.23
12.00	350.46	2079.7	198.96	4332.9	3081.5	-26553	-1103.0	9343.3	609.78
12.25	333.89	2060.7	255.67	5692.8	4350.0	-28735	-1783.4	8970.1	370.20
12.50	326.75	2371.7	354.88	7117.4	4941.8	-31866	-2509.9	9430.2	150.43

Table 7. The Values $10^{-3} \times b540_j(x_0)$ for $-5 \leq j \leq 3$ Calculated With a Step $\Delta x_0 = 0.25$ in the Dimensionless Height Range $2 \leq x_0 \leq 12.5$

x_0	j								
	-5	-4	-3	-2	-1	0	1	2	3
2.00	2.97	0.00	7.26	82.40	46.78	-268.96	8.87	22.64	26.98
2.25	3.12	0.00	9.66	87.26	45.58	-281.13	6.53	30.57	25.61
2.50	3.46	0.00	13.78	91.77	42.05	-295.81	2.47	32.87	26.46
2.75	3.94	0.00	20.60	91.75	30.58	-292.39	-2.57	26.49	28.01
3.00	4.35	0.00	28.81	87.36	21.48	-284.67	-6.35	21.03	28.62
3.25	2.00	4.05	31.96	84.07	16.20	-279.09	-8.62	18.72	28.41
3.50	2.36	5.60	31.03	82.42	13.92	-275.99	-10.28	19.28	27.42
3.75	2.67	7.54	27.73	81.71	11.96	-271.48	-11.90	20.90	25.92
4.00	2.99	10.19	24.97	82.25	9.08	-268.78	-13.76	22.86	24.61
4.25	3.36	13.64	24.06	85.28	5.74	-273.39	-16.34	25.18	24.06
4.50	3.79	17.35	24.74	89.87	2.84	-284.70	-20.18	29.25	23.55
4.75	4.25	20.53	26.52	94.19	-0.20	-297.13	-24.84	33.54	23.04
5.00	4.76	23.45	28.85	97.93	-3.37	-311.12	-29.37	38.84	22.24
5.25	5.24	25.81	30.78	100.04	-6.42	-321.10	-33.39	43.88	21.21
5.50	5.70	28.05	31.61	100.25	-9.25	-324.51	-36.67	48.01	19.90
5.75	6.14	30.36	31.87	101.51	-10.76	-331.54	-39.52	53.00	18.82
6.00	6.59	33.05	31.92	103.96	-10.60	-344.29	-41.92	58.97	18.36
6.25	6.97	35.93	32.19	108.17	-8.91	-363.74	-44.28	65.94	18.63
6.50	9.51	32.67	35.52	114.52	-5.91	-390.00	-47.09	73.91	19.69
6.75	13.03	28.27	39.67	122.72	-1.95	-421.49	-50.49	82.20	21.62
7.00	18.17	23.39	44.58	133.80	2.93	-461.42	-54.86	91.18	24.81
7.25	25.31	18.72	50.23	148.85	8.62	-512.36	-60.51	101.39	29.44
7.50	33.63	14.75	56.23	167.36	14.93	-570.45	-67.28	112.17	35.06
7.75	39.98	11.96	61.76	187.44	20.14	-626.74	-73.83	119.34	43.08
8.00	44.11	10.70	68.46	214.00	23.26	-695.95	-82.14	125.66	55.47
8.25	47.27	10.74	77.89	250.24	22.43	-785.21	-93.71	131.64	73.65
8.50	50.26	12.32	91.51	298.71	15.72	-900.03	-109.84	137.32	97.26
8.75	53.38	16.00	110.25	360.30	1.65	-1042.8	-131.04	142.63	125.72
9.00	56.54	22.08	135.02	425.40	-19.36	-1201.7	-154.97	146.20	156.67
9.25	59.67	31.33	167.12	487.60	-52.50	-1372.1	-179.21	154.91	185.00
9.50	63.13	44.31	205.38	500.36	-88.32	-1500.9	-195.44	162.86	200.60
9.75	67.25	61.35	249.81	518.66	-173.93	-1607.9	-216.16	205.14	184.21
10.00	72.52	87.08	300.32	497.95	-193.74	-1748.8	-251.54	252.70	141.08
10.25	78.56	120.85	343.69	505.59	-270.72	-1899.5	-286.33	326.97	109.54
10.50	86.09	167.90	369.76	437.87	-251.73	-2023.5	-332.52	370.66	79.72
10.75	96.43	233.15	339.02	394.61	-254.55	-2205.9	-363.08	447.00	80.95
11.00	109.46	322.89	305.83	386.25	-255.79	-2515.6	-414.51	572.53	78.42

Table 7. (continued)

x_0	j								
	-5	-4	-3	-2	-1	0	1	2	3
11.25	126.92	448.86	302.44	426.15	-318.44	-3125.5	-469.24	823.40	110.46
11.50	144.41	582.43	275.41	471.82	-336.49	-3718.5	-510.67	1044.0	142.77
11.75	159.16	674.02	180.70	550.47	-293.24	-4216.4	-514.34	1242.7	158.64
12.00	160.12	723.80	114.75	715.11	-69.80	-4691.4	-541.51	1330.2	110.12
12.25	154.71	704.19	113.10	885.68	24.90	-4676.8	-633.12	1171.3	64.98
12.50	150.21	790.25	117.79	1050.7	117.71	-4950.7	-685.70	1195.5	23.63

Table 8. The Values $10^{-1} \times a720_j(x_0)$ for $-5 \leq j \leq 3$ Calculated With a Step $\Delta x_0 = 0.25$ in the Dimensionless Height Range $2 \leq x_0 \leq 12.5$

x_0	j								
	-5	-4	-3	-2	-1	0	1	2	3
2.00	1.10	0.00	8.16	280.44	538.98	-1528.6	138.91	330.52	50.98
2.25	1.54	0.00	13.68	369.55	575.60	-1814.7	135.96	395.57	69.20
2.50	1.99	0.00	22.56	470.49	620.84	-2148.6	119.61	451.37	94.59
2.75	2.43	0.00	36.56	577.23	660.36	-2494.9	99.21	482.26	124.17
3.00	2.88	0.00	58.20	691.63	683.25	-2832.2	64.25	491.44	156.22
3.25	0.49	4.48	84.54	825.27	675.46	-3164.1	23.65	497.22	187.64
3.50	0.76	7.66	114.94	955.96	637.00	-3453.8	-12.94	511.43	212.63
3.75	1.11	12.92	144.65	1070.0	591.60	-3696.8	-51.50	538.44	229.95
4.00	1.51	20.68	170.88	1171.0	543.64	-3905.6	-92.07	576.32	239.14
4.25	1.88	30.26	196.41	1260.6	499.93	-4096.0	-131.52	617.98	242.31
4.50	2.24	40.80	225.43	1338.3	467.38	-4276.3	-169.92	662.11	240.71
4.75	2.60	52.14	265.60	1411.4	442.87	-4472.6	-219.95	708.89	238.55
5.00	2.98	66.46	316.64	1480.9	406.45	-4684.3	-265.37	764.37	236.13
5.25	3.37	83.83	366.16	1543.0	377.27	-4905.4	-309.09	830.82	235.74
5.50	3.77	105.12	408.75	1612.0	358.18	-5152.9	-354.43	909.33	239.20
5.75	4.23	130.36	441.96	1688.1	346.71	-5422.9	-404.49	995.46	246.79
6.00	4.75	159.65	469.12	1769.2	340.59	-5705.3	-460.35	1082.3	257.94
6.25	5.36	193.02	494.02	1856.4	337.80	-6004.2	-519.11	1166.5	272.44
6.50	7.92	222.83	522.69	1956.4	343.43	-6332.4	-578.58	1252.2	290.22
6.75	11.95	249.59	555.84	2070.3	361.85	-6702.7	-635.85	1340.2	313.00
7.00	18.39	271.46	594.41	2196.7	398.00	-7123.3	-689.30	1430.0	342.42
7.25	27.90	288.63	639.37	2337.2	453.27	-7606.6	-736.42	1525.0	377.69
7.50	40.91	304.43	691.46	2498.1	533.38	-8171.1	-778.25	1627.2	422.87
7.75	55.65	323.69	749.69	2690.2	635.84	-8852.2	-816.32	1740.0	489.89
8.00	67.75	346.39	810.44	2911.6	749.37	-9620.1	-847.97	1860.1	584.74
8.25	76.42	373.51	875.28	3166.9	871.09	-10484	-876.88	1990.9	715.38
8.50	83.22	405.55	946.81	3456.0	1004.7	-11462	-909.31	2135.1	879.35
8.75	91.30	442.97	1029.0	3786.4	1144.5	-12584	-953.91	2289.7	1078.6
9.00	101.64	487.21	1124.9	4087.8	1276.7	-13731	-999.25	2414.9	1308.4
9.25	114.15	538.15	1229.3	4294.1	1287.7	-14705	-1011.0	2528.8	1508.4
9.50	129.75	598.19	1322.6	4058.5	1173.9	-14918	-935.69	2552.6	1579.5
9.75	148.28	672.70	1408.3	3925.2	621.24	-15042	-845.80	2997.2	1333.4
10.00	170.53	762.00	1468.2	3618.3	591.49	-15116	-939.69	3281.7	900.65
10.25	192.76	869.04	1452.3	3575.1	240.91	-15492	-1015.6	3941.9	493.38
10.50	214.51	1004.0	1369.8	3182.0	711.13	-15760	-1139.7	3973.7	347.62
10.75	244.69	1185.9	1094.4	2949.4	884.40	-16440	-998.82	4402.0	467.28
11.00	284.11	1437.6	884.20	3026.1	1258.9	-18408	-933.12	5268.2	645.06
11.25	332.74	1780.5	833.15	3413.2	1395.3	-22590	-720.06	7670.8	845.41
11.50	375.93	2129.6	743.82	3778.8	1752.5	-26251	-677.51	9556.2	974.09
11.75	402.15	2314.6	446.73	3998.0	1966.5	-28011	-624.91	10617	971.24
12.00	376.15	2327.8	242.01	4581.0	2999.8	-28413	-1116.4	9895.3	637.35
12.25	372.40	2358.8	201.06	6059.6	4673.2	-31152	-1761.4	9460.6	344.89
12.50	379.61	2675.5	230.96	7776.3	5770.9	-35374	-2440.1	10057	87.50

Table 9. The Values $10^{-3} \times b720_j(x_0)$ for $-5 \leq j \leq 3$ Calculated With a Step $\Delta x_0 = 0.25$ in the Dimensionless Height Range $2 \leq x_0 \leq 12.5$

x_0	j								
	-5	-4	-3	-2	-1	0	1	2	3
2.00	2.84	0.00	7.49	87.26	49.15	-283.06	10.23	21.83	29.34
2.25	3.04	0.00	10.13	93.39	49.06	-299.80	8.40	31.44	27.75
2.50	3.44	0.00	14.77	99.68	47.20	-322.28	4.68	35.81	28.84
2.75	3.98	0.00	22.24	101.62	38.19	-329.51	-0.36	31.37	31.07
3.00	4.46	0.00	31.28	97.14	27.68	-321.13	-4.80	24.67	32.10
3.25	1.99	4.30	34.96	92.32	19.55	-308.63	-7.87	20.41	31.87
3.50	2.36	6.00	34.16	90.10	16.57	-303.84	-9.94	20.70	30.83
3.75	2.70	8.16	30.61	89.62	14.40	-299.82	-11.98	22.59	29.27
4.00	3.04	11.08	27.70	91.66	11.56	-300.89	-14.40	25.52	28.02
4.25	3.42	14.89	26.88	96.04	8.00	-308.85	-17.50	28.63	27.57
4.50	3.86	19.00	27.89	102.25	4.85	-324.37	-22.10	33.74	27.15
4.75	4.35	22.60	30.26	108.26	1.46	-341.45	-27.81	39.19	26.72
5.00	4.87	25.86	33.16	113.40	-2.18	-359.46	-33.26	45.53	25.94
5.25	5.38	28.56	35.61	116.71	-5.69	-373.09	-38.15	51.59	24.86
5.50	5.86	31.11	36.90	117.84	-9.11	-379.11	-42.33	56.61	23.38
5.75	6.33	33.72	37.27	118.91	-11.69	-384.88	-45.89	61.65	21.87
6.00	6.80	36.90	37.60	121.74	-12.07	-399.08	-48.83	68.10	21.05
6.25	7.22	40.33	38.37	127.12	-10.37	-423.20	-51.74	76.31	20.95
6.50	9.86	37.43	42.37	134.71	-6.81	-455.32	-54.98	85.86	21.69
6.75	13.56	33.32	47.18	144.19	-1.74	-493.73	-58.66	95.89	23.54
7.00	18.96	28.66	52.63	156.48	4.70	-540.94	-63.18	106.69	26.81
7.25	26.43	24.08	58.63	172.85	12.58	-599.82	-68.83	119.02	31.51
7.50	35.15	20.13	65.02	193.28	21.79	-667.85	-75.63	132.44	37.24
7.75	41.83	17.32	70.90	216.18	30.62	-736.75	-82.38	142.90	45.58
8.00	46.29	16.07	78.13	246.82	38.08	-822.74	-91.16	153.61	58.73
8.25	49.88	16.07	88.23	288.24	42.52	-932.98	-103.44	165.15	78.53
8.50	53.23	17.74	102.55	343.31	41.67	-1073.2	-120.83	176.96	105.53
8.75	56.58	21.72	122.20	413.97	33.03	-1246.5	-144.27	188.02	139.75
9.00	59.32	28.29	147.33	487.33	15.63	-1430.1	-170.16	194.33	177.88
9.25	62.25	38.01	180.11	557.12	-18.40	-1619.4	-196.22	203.77	213.56
9.50	65.58	51.42	218.82	566.68	-58.78	-1745.3	-211.94	211.81	232.10
9.75	69.61	68.20	263.12	590.63	-157.44	-1852.4	-233.19	260.85	211.70
10.00	75.22	94.38	318.88	584.41	-189.82	-2027.6	-280.95	327.30	158.52
10.25	81.82	129.71	368.27	619.14	-281.65	-2242.0	-343.55	437.37	105.53
10.50	89.63	178.00	403.74	552.18	-260.89	-2410.2	-401.73	464.32	86.12
10.75	100.36	246.47	376.01	497.80	-279.95	-2605.3	-424.44	519.42	112.74
11.00	114.49	341.57	350.45	481.10	-295.72	-2946.2	-467.15	618.40	147.15
11.25	132.73	474.33	362.99	520.29	-386.60	-3636.4	-530.04	911.63	185.27
11.50	150.94	615.56	347.10	562.21	-420.73	-4235.3	-589.04	1155.9	200.12
11.75	165.68	713.79	241.18	617.35	-399.48	-4634.7	-592.24	1350.8	189.77
12.00	165.99	767.11	152.53	759.90	-201.22	-4931.6	-626.92	1372.1	126.98
12.25	164.00	763.27	119.05	956.20	-50.09	-5031.6	-700.61	1212.4	66.34
12.50	165.39	869.58	90.84	1175.3	88.08	-5475.1	-763.86	1258.9	21.10

$$\Phi(x) = \tilde{\varepsilon}(x) + \varphi(x) \quad (14)$$

is the boundary condition to be determined at the level $x = 16.5$ from the recurrence equation (9).

7. Summary

A new parameterization for evaluation of the cooling rate of the middle and upper atmosphere for the 15 μm CO₂ band has been developed. The parameterization is based on the matrix-recurrence relationship approach and provides very high computational efficiency. Parameterization formulae provide an explicit dependence

of the cooling rate on temperature, atmospheric composition (excluding CO₂), and quenching rate constants. To take into account the dependence on CO₂ concentration, a method for interpolation of the parameterization coefficients has been developed. The parameterization is valid over a wide range of CO₂ concentrations (150–720 ppm). Because of its high computational efficiency, the parameterization is primarily recommended to be used in comprehensive 3-D atmospheric models, especially those where NLTE treatment is required.

The accuracy of the method has been examined for a wide variety of atmospheric conditions. The parameterization provides quite satisfactory agreement with

Table 10. Dependence of Escape Function $L(u)$ on the Total CO₂ Column Amount u

$\log(u)$	$-\log[L(u)]$	$\log(u)$	$-\log[L(u)]$
< 26.3216	0	36.8923	1.78857
26.3216	2.41011-4	37.1960	2.08170
27.0882	5.47141-4	37.4904	2.37948
27.7324	1.06159-3	37.7763	2.67572
28.3000	1.87979-3	38.0552	2.96732
28.8270	3.16602-3	38.3278	3.25212
29.3322	5.18544-3	38.5950	3.53048
29.8124	8.21667-3	38.8582	3.80372
30.2630	1.25089-2	39.1183	4.07275
30.6894	1.83860-2	39.3762	4.33831
31.0997	2.63111-2	39.6322	4.60105
31.4990	3.68818-2	39.8869	4.86159
31.8925	5.09649-2	40.1406	5.12037
32.2872	7.00406-2	40.3934	5.37779
32.6843	9.60375-2	40.6456	5.63412
33.0779	1.30768-1	40.8973	5.88939
33.4646	1.76295-1	41.1486	6.14349
33.8430	2.35023-1	41.3997	6.39644
34.2120	3.09521-1	41.6505	6.64877
34.5720	4.02734-1	41.9011	6.90146
34.9237	5.17857-1	42.1516	7.15521
35.2679	6.58126-1	42.4020	7.40965
35.6054	8.26500-1	42.6523	7.66354
35.9362	1.02468	42.9025	7.91568
36.2610	1.25290	43.1527	8.16587
36.5801	1.50947	43.4028	8.41502

Read 2.41011-4 as 2.41011×10^{-4} ; u is in cm^{-2} .

benchmark reference (line-by-line) calculations over all height and latitudinal regions. For the 360 ppm CO₂ model the error does not exceed 0.3, 1.6, and 1 K d⁻¹ in the height regions below $x = 11$ ($z \approx 76$ km), between $x = 11$ and $x = 14$, and above $x = 14$ ($z \approx 93$ km), respectively. For the double CO₂ concentration (720 ppm) the error, in the same height regions, can reach 0.5, 5, and 3 K d⁻¹, respectively. For the halved (150 ppm) CO₂ concentration the error does not exceed ~ 0.5 K d⁻¹ throughout all the domain. These maximum errors occur in the narrow Subarctic region during the summer season, and errors are much less for other regions and seasons. For arbitrary CO₂ concentrations the parameterization approximates the cooling rate values with the same accuracy as it does for the basic CO₂ models. In the NLTE layer the scheme provides an appropriate response to variations in the atomic oxygen concentration.

Two versions of the parameterization, with uniform (full) and optimized height grids, have been developed. Employing the method of matrix transformation suggested by Akmaev and Fomichev [1992], the uniform grid parameterization can be adopted for any vertical coordinate grid used in a given dynamical model. In the present study we utilized this method in order to optimize the parameterization by minimizing the number of levels which contribute to the cooling rate at a given level as well as the number of parameterization coefficients. With the optimized grid, only eight

Table 11. Dependence of Values $\alpha(u, x_j)$ on the Total CO₂ Column Amount $u(x_j)$ Calculated in the Dimensionless Height Range $12.50 \leq x_j \leq 13.75$ With a Step $\Delta x_j = 0.25$

x_j	$\log(u(x_j))$	$\alpha(u, x_j)$
12.50	36.9008	1.28799
	37.7763	1.62387
	38.1817	1.87071
12.75	38.4694	2.06443
	36.6149	1.22735
	37.4904	1.52566
	37.8958	1.70450
13.00	38.1835	1.85887
	36.3206	1.11078
	37.1960	1.34421
	37.6015	1.45841
13.25	37.8892	1.57233
	36.0168	1.09607
	36.8923	1.22971
	37.2977	1.29592
13.50	37.5854	1.35612
	35.7046	1.04633
	36.5801	1.13247
	36.9855	1.16349
13.75	37.2732	1.19569
	35.3855	1.03442
	36.2610	1.05963
	36.6665	1.07132
	36.9541	1.08278

The $u(x_j)$ are in cm^{-2} .

levels need to be considered to account for the internal heat exchange in the LTE region of the atmosphere. The parameterization coefficients for the optimized grid are presented in the paper. Tables 2-9 are also available from anonymous ftp at maia.sca.uqam.ca (132.208.133.174) in the file pub/CO2param/CO2tab. The parameterization coefficients for the optimized or the full height grid can also be obtained upon request from the principal author (VIF).

Acknowledgments. The authors would like to thank W. E. Ward and J. C. McConnell for their useful comments, which are highly appreciated. This work has been supported by the Canadian MAM project, through grants from the Natural Sciences and Engineering Research Council and the Atmospheric Environment Service of Canada.

References

- Akmaev, R. A., and V. I. Fomichev, Adaptation of a matrix parameterization of the middle atmosphere radiative cooling for an arbitrary vertical coordinate grid, *J. Atmos. Terr. Phys.*, **54**, 829-833, 1992.
- Akmaev, R. A., and G. M. Shved, Parameterization of the radiative flux divergence in the 15 μm CO₂ band in the 30-75 km layer, *J. Atmos. Terr. Phys.*, **44**, 993-1004, 1982.
- Akmaev, R. A., V. I. Fomichev, N. M. Gavrilov, and G. M. Shved, Simulations of the zonal mean climatology of the middle atmosphere with a three-dimensional spectral model for solstice and equinox conditions, *J. Atmos. Terr. Phys.*, **54**, 119-128, 1992.

- Andrews, D. G., J. R. Holton, and C. B. Leovy, *Middle Atmosphere Dynamics*, 489 pp., Academic, San Diego, Calif., 1987.
- Apruzese, J. P., D. F. Strobel, and M. R. Schoeberl, Parameterization of IR cooling in a middle atmosphere dynamics model, 2, Non-LTE radiative transfer and the globally averaged temperature of the mesosphere and lower thermosphere, *J. Geophys. Res.*, **89**, 4917-4926, 1984.
- Beagley, S. R., J. de Grandpre, J. N. Koshyk, N. A. McFarlane, and T. G. Shepherd, Radiative-dynamical climatology of the first-generation Canadian Middle Atmosphere Model, *Atmos. Ocean*, **35**, 293-331, 1997.
- Berger, U., and M. Dameris, Cooling of the upper atmosphere due to CO₂ increases: A model study, *Ann. Geophys.*, **11**, 809-819, 1993.
- Bougher, S. W., D. M. Hunten, and R. G. Roble, CO₂ cooling in terrestrial planet thermospheres, *J. Geophys. Res.*, **99**, 14,609-14,622, 1994.
- Briegleb, B. P., Longwave band model for thermal radiation in climate studies, *J. Geophys. Res.*, **97**, 11,475-11,485, 1992.
- Chamberlain, J. W., and D. M. Hunten, *Theory of Planetary Atmospheres*, 481 pp., Academic, San Diego, Calif., 1987.
- Chen, L., J. London, and G. Brasseur, Middle atmospheric ozone and temperature responses to solar irradiance variations over 27-day period, *J. Geophys. Res.*, **102**, 29,957-29,979, 1997.
- Chou, M.-D., and L. Kouvaris, Calculations of transmission functions in the infrared CO₂ and O₃ bands, *J. Geophys. Res.*, **96**, 9003-9012, 1991.
- Drummond, J. R., J. Cormier, and Z. Yu, *General Atmospheric Spectral Integration Suite: GENASIS User Manual*, Dep. of Phys., Univ. of Toronto, Ontario, Can., 1993.
- Fels, S. B., J. D. Mahlman, M. D. Schwarzkopf, and R. W. Sinclair, Stratospheric sensitivity to perturbations in ozone and carbon dioxide: Radiative and dynamical response, *J. Atmos. Sci.*, **37**, 2265-2297, 1980.
- Fleming, E. L., S. Chandra, J. J. Barnett, and M. Corney, Zonal mean temperature, pressure, zonal wind and geopotential height as functions of latitude, *Adv. Space Res.*, **10**, (12)11-(12)59, 1990.
- Fomichev, V. I., and J.-P. Blanchet, Development of the new CCC/GCM radiation model for extension into the middle atmosphere, *Atmos. Ocean*, **33**, 513-529, 1995.
- Fomichev, V. I., A. A. Kutepov, R. A. Akmaev, and G. M. Shved, Parameterization of the 15 μm CO₂ band cooling in the middle atmosphere (15-115 km), *J. Atmos. Terr. Phys.*, **55**, 7-18, 1993.
- Fomichev, V. I., W. E. Ward, and C. McLandress, Implications of variations in the 15 μm CO₂ band cooling in the mesosphere and lower thermosphere associated with current climatologies of the atomic oxygen mixing ratio, *J. Geophys. Res.*, **101**, 4041-4055, 1996.
- Grinkevich, I. Ya., and V. I. Fomichev, Comparison of radiative cooling parameterizations for the stratosphere and mesosphere, *Atmos. Oceanic Phys.*, **29**, 340-345, 1993.
- Haus, R., Accurate cooling rates of the 15 μm CO₂ band: Comparison with recent parameterizations, *J. Atmos. Terr. Phys.*, **48**, 559-561, 1986.
- Hedin, A. E., Extension of the MSIS thermospheric model into the middle and lower atmosphere, *J. Geophys. Res.*, **96**, 1159-1172, 1991.
- Kiehl, J. T., and B. P. Briegleb, A new parameterization of the absorptance due to the 15 μm band system of carbon dioxide, *J. Geophys. Res.*, **96**, 9013-9019, 1991.
- Kutepov, A. A., and V. I. Fomichev, Application of the second-order escape probability approximation to the solution of the NLTE vibration-rotation band radiative transfer problem, *J. Atmos. Terr. Phys.*, **55**, 1-6, 1993.
- Kutepov, A. A., and G. M. Shved, Radiative transfer in the 15 μm CO₂ band with the breakdown of local thermodynamic equilibrium in the Earth's atmosphere, *Atmos. Oceanic Phys.*, **14**, 18-30, 1978.
- Llewellyn, E. J., I. C. McDade, and M. D. Lockerie, Proposed reference models for atomic oxygen in the terrestrial atmosphere, *MAP Handb.*, **31**, 139-154, 1989.
- Lopez-Puertas M., M. A. Lopez-Valverde, C. P. Rinsland, and M. R. Gunson, Analysis of upper atmosphere CO₂(ν_2) vibrational temperature retrieved from ATMOS/Spacelab 3 observation, *J. Geophys. Res.*, **97**, 20,469-20,478, 1992.
- Morcrette, J.-J., Sur la parameterisation du rayonnement dans les modeles de la circulation generale atmospherique, Ph.D. thesis, 373 pp., Univ. des Sci. et Tech. de Lille, Lille, France, 1984.
- Offermann, D., V. Friedrich, P. Ross, and U. von Zahn, Neutral gas composition measurements between 80 and 120 km, *Planet. Space Sci.*, **29**, 747-764, 1981.
- Ogibalov, V. P., V. I. Fomichev, and A. A. Kutepov, The NLTE radiative flux divergences in the 15 μm CO₂ band, paper presented at 8th Scientific Assembly, Int. Assoc. of Geomagn. and Aeron., Uppsala, Sweden, Aug. 4-14, 1997.
- Ogibalov, V. P., A. A. Kutepov, and G. M. Shved, Non-local thermodynamic equilibrium in CO₂ in the middle atmosphere, II, Populations of the $\nu_1\nu_2$ modes manifold states, *J. Atmos. Sol. Terr. Phys.*, **60**, 315-329, 1998.
- Pollock, D. S., G. B. I. Scott, and L. F. Phillips, Rate constant for quenching of CO₂(010) by atomic oxygen, *Geophys. Res. Lett.*, **20**, 727-729, 1993.
- Rinsland, C. P., M. R. Gunson, R. Zander, and M. Lopez-Puertas, Middle and upper atmosphere pressure-temperature profiles and the abundances of CO₂ and CO in the upper atmosphere from ATMOS/Spacelab 3 observations, *J. Geophys. Res.*, **97**, 20,479-20,495, 1992.
- Rishbeth, H., and R. G. Roble, Cooling of the upper atmosphere by enhanced greenhouse gases: Modelling of thermospheric and ionospheric effects, *Planet. Space Sci.*, **40**, 1011-1026, 1992.
- Roble, R. G., and E. C. Ridley, A thermosphere-ionosphere-mesosphere-electrodynamics general circulation model (time-GCM): Equinox solar minimum simulations (30-500 km), *Geophys. Res. Lett.*, **21**, 417-420, 1994.
- Rothman, L. S., AFGL atmospheric absorption line parameters compilation: 1980 version, *Appl. Opt.*, **20**, 791-795, 1981.
- Rothman, L. S., et al., The HITRAN molecular database: Edition of 1991 and 1992, *J. Quant. Spectrosc. Radiat. Transfer*, **48**, 469-507, 1992.
- Schwarzkopf, M. D., and S. B. Fels, Improvements to the algorithm for computing CO₂ transmissivities and cooling rates, *J. Geophys. Res.*, **90**, 10,541-10,550, 1985.
- Shved, G. M., L. E. Khvorostovskaya, I. Yu. Potekhin, A. I. Demyanikov, A. A. Kutepov, and V. I. Fomichev, Measurements of the quenching rate constant for collisions CO₂ (01¹0)-O: The importance of rate constant magnitude for the thermal regime and radiation of the lower thermosphere, *Atmos. Oceanic Phys.*, **27**, 295-299, 1991.
- Shved, G. M., A. A. Kutepov, and V. P. Ogibalov, Non-local thermodynamic equilibrium in CO₂ in the middle atmosphere, I, Input data and populations of the ν_3 mode manifold states, *J. Atmos. Sol. Terr. Phys.*, **60**, 289-314, 1998.
- Trinks, H., and K. H. Fricke, Carbon dioxide concentrations in the lower thermosphere, *J. Geophys. Res.*, **83**, 3883-3886, 1978.

- Wehrbein, W. M., and C. B. Leovy, An accurate radiative heating and cooling algorithm for use in a dynamical model of the middle atmosphere, *J. Atmos. Sci.*, **39**, 1532-1544, 1982.
- Zhu, X., Carbon dioxide 15 μm band cooling rates in the upper middle atmosphere calculated by Curtis matrix interpolation, *J. Atmos. Sci.*, **47**, 755-774, 1990.
- Zhu, X., An accurate and efficient radiation algorithm for middle atmosphere model, *J. Atmos. Sci.*, **51**, 3593-3614, 1994.
- town", Montréal, Québec, Canada H3C 3P8. (e-mail: blanchet.jean-pierre@uqam.ca)
- V. I. Fomichev, Department of Earth and Atmospheric Science, York University, 4700 Keele Street, Toronto, Ontario, Canada M3J 1P3. (e-mail: victor@nimbus.yorku.ca)
- D. S. Turner, Meteorological Research Branch, Atmospheric Environment Service, 4905 Dufferin Street, Environment Service, 4905 Dufferin Street, Toronto, Ontario, Canada M3H 5T4. (e-mail: sturner@smarts6.tor.ec.gc.ca)

J.-P. Blanchet, Earth Sciences Department, Université du Québec à Montréal, P.O. Box 8888, Station "Down-

(Received October 29, 1997; revised March 3, 1998; accepted March 6, 1998.)